Journal of Medicinal Chemistry

Article

Identification of N-{cis-3-[Methyl(7H-pyrrolo[2,3-d]pyrimidin-4-yl)amino]cyclobutyl}propane-1-sulfonamide (PF-04965842): A Selective JAK1 Clinical Candidate for the Treatment of Autoimmune Diseases

Michael L Vazquez, Neelu Kaila, Joseph W Strohbach, John D Trzupek, Matthew F. Brown, Mark E. Flanagan, Mark J MItton-Fry, Timothy A Johnson, Ruth E TenBrink, Eric P Arnold, Arindrajit Basak, Steven E Heasley, Soojin Kwon, Jonathan Langille, Mihir D. Parikh, Sarah H Griffin, Jeffrey M. Casavant, Brian A Duclos, Ashley E Fenwick, Thomas M Harris, Seungil Han, Nicole L. Caspers, Martin E. Dowty, Xin Yang, Mary Ellen Banker, Martin Hegen, Peter T. Symanowicz, Li Li, Lu Wang, Tsung H. Lin, Jason Jussif, James D Clark, Jean-Baptiste Telliez, Ralph P. Robinson, and Ray Unwalla

J. Med. Chem., **Just Accepted Manuscript** • Publication Date (Web): 03 Jan 2018

Just Accepted

ACS Publications

Journal of Medicinal Chemistry is published by the American Chemical Society. 1155 Sixteenth Street N.W., Washington, DC 20036

	Robinson, Ralph; Pfizer Inc, PGRD Unwalla, Ray; Pfizer Research and Development, World wide Medicinal Chemistry

Identification of *N*-{*cis*-3-[Methyl(7*H*-pyrrolo[2,3-*d*]pyrimidin-4-yl)amino]cyclobutyl}propane-1-sulfonamide (PF-04965842): A Selective JAK1 Clinical Candidate for the Treatment of Autoimmune Diseases

Michael L. Vazquez[†], *Neelu Kaila*[†], *Joseph W. Strohbach*[†], *John D. Trzupek*[†], *Matthew F. Brown*[‡], *Mark E. Flanagan*[‡], *Mark J. Mitton-Fry*[‡], *Timothy A. Johnson, Ruth E. TenBrink, Eric P. Arnold*[‡], *Arindrajit Basak, Steven E. Heasley*[‡], *Soojin Kwon*[‡], *Jonathan Langille*[‡], *Mihir D. Parikh*[‡], *Sarah H. Griffin*[§], *Jeffrey M. Casavant*[‡] , *Brian A. Duclos, Ashley E. Fenwick, Thomas M. Harris*[‡], *Seungil Han*[‡], *Nicole Caspers*[‡], *Martin, E. Dowty*[‖], *Xin Yang*[‡], *Mary Ellen Banker*[‡], *Martin Hegen*[#], *Peter T. Symanowicz*[#], *Li Li*[#], *Lu Wang*[#], *Tsung H. Lin*[#], *Jason Jussif*[#], *James D. Clark*[#], *Jean-Baptiste Telliez*[#], *Ralph P. Robinson*[‡]* *and Ray Unwalla*[†]*

[†]Medicine Design, Pfizer Inc, 610 Main Street, Cambridge, MA 02139

[‡]Medicine Design, Pfizer Inc, Eastern Point Road, Groton, CT 06340

[§]Chemical Research Development, Pfizer Inc, Eastern Point Road, Groton, CT 06340

[‖]Medicine Design, Pfizer Inc, 1 Burtt Rd, Andover, MA 01810

[#]Inflammation and Immunology, Pfizer Inc, 610 Main Street, Cambridge, MA 02139

*Corresponding authors: ralph.p.robinson@pfizer.com and ray.unwalla@pfizer.com

ABSTRACT: Janus kinases (JAKs) are intracellular tyrosine kinases that mediate the signaling of numerous cytokines and growth factors involved in the regulation of immunity, inflammation and hematopoiesis. As JAK1 pairs with JAK2, JAK3 and TYK2, a JAK1-selective inhibitor would be expected to inhibit many cytokines involved in inflammation and immune function, while avoiding inhibition of the JAK2 homodimer regulating erythropoietin (EPO) and

thrombopoietin (TPO) signaling. Our efforts began with tofacitinib, an oral JAK inhibitor approved for the treatment of rheumatoid arthritis (RA). Through modification of the 3-aminopiperidine linker in tofacitinib, we discovered highly selective JAK1 inhibitors with nanomolar potency in a human whole blood assay. Improvements in JAK1 potency and selectivity were achieved via structural modifications suggested by X-ray crystallographic analysis. After demonstrating efficacy in a rat adjuvant-induced arthritis (rAIA) model, PF-04965842 (**25**) was nominated as a clinical candidate for the treatment of JAK1-mediated autoimmune diseases.

INTRODUCTION

Janus kinases (JAKs) are intracellular tyrosine kinases that mediate the signaling of numerous cytokines and growth factors involved in the regulation of immunity, inflammation and hematopoiesis.[1] There are four members of the Janus kinase family: JAK1, JAK2, JAK3 and TYK2. A cytokine binding to its receptor initiates the dimerization or multimerization of receptor units. JAKs associated with the receptor subunits are brought into proximity resulting in their phosphorylation and activation. The activated JAKs in turn phosphorylate specific tyrosine residues within the intracellular domain of the cytokine receptor. These phosphorylated tyrosine residues create docking sites for the recruitment and phosphorylation of signal transducers and activators of transcription (STAT) proteins. Subsequently, the STATs dimerize and translocate to the cell nucleus where they modulate gene expression.[2]

JAK1 has the broadest cytokine signaling profile amongst the JAK family members and is the only isoform that pairs with the other three JAKs. In combination with JAK3, which pairs only with JAK1, it regulates the signaling of the gamma common (γ_c) cytokines. JAK1 pairing specifically with JAK2 regulates signaling of type II interferon (IFNγ). JAK1 paired with TYK2 regulates signaling of type I interferons (IFNα, IFNβ) and the IL-10 family of cytokines.[3] Additionally, when paired with JAK2 or TYK2, JAK1 regulates signaling of gp130-containing receptors (including the prototypic cytokine IL-6 receptor) as well as signaling through the granulocyte macrophage colony-stimulating factor (GM-CSF) receptor.[4] JAK1-independent cytokines include IL-12 and IL-23 whose receptors signal via JAK2 and TYK2. JAK2 is the only member of the family that pairs with itself, regulating signals for various cytokines and growth factors including IL-3, IL-5, GM-CSF, EPO and TPO.[5] There are no redundant pathways known for cytokines that signal through the JAKs and many of these cytokines have been implicated in a number of autoimmune diseases, making them attractive drug targets.[1e,6]

Tofacitinib (**1**) (Figure 1), a JAK1/JAK3 inhibitor with moderate activity on JAK2 and baricitinib (**2**) a JAK1/JAK2 inhibitor are approved for the treatment of rheumatoid arthritis (RA).[7,8] Ruxolitinib (**3**), which inhibits both JAK1 and JAK2, is approved for the treatment of primary myelofibrosis (PMF).[9] Tofacitinib and baricitinib are also in clinical trials for other autoimmune indications.[10] Since these compounds have activity against JAK2, the potential for anemia and thrombocytopenia exists due to interference with EPO and TPO signaling. In Phase 2 dose ranging-studies, reduction in hemoglobin was observed in patients treated with baricitinib and tofacitinib.[10,11]

[Figure 1]

Based on human genetic data, the loss of JAK3 function through mutation results in severe combined immunodeficiency (SCID) due to the loss in signaling of the γ_c cytokines.[1] The SCID clinical phenotype resulting from JAK3 inactivating mutations essentially identical to the X-linked SCID phenotype resulting from inactivating mutations in the γ_c receptor chain.[12] As such, JAK3 has been a target of interest for the treatment of transplant rejection and other immune disorders including RA. Since inhibition of transplant rejection was a focus during the initial drug discovery program leading to the discovery of tofacitinib, JAK3 was of particular interest due to its role in controlling common γ-chain cytokine signaling and because of its known expression, which is restricted to lymphoid cells. [13] However, with the development of improved kinase assays, the pan-JAK (i.e., non-selective) inhibitory nature of tofacitinib within the JAK family was ultimately revealed and with it the recognition that JAK1 inhibition is a major contributor to its pharmacology.[14] In light of these findings, we initiated a program to discover and develop a potent and selective JAK1 inhibitor.[2,15,16] As JAK1 pairs with JAK2, JAK3 and TYK2, a JAK1-selective inhibitor would be expected to inhibit many cytokines involved in inflammation and immune function, while avoiding the inhibition of the JAK2 homodimer regulating EPO and TPO signaling and other cytokines.[17] Herein we describe the identification and characterization of a novel series of potent and orally bioavailable small molecule inhibitors of JAK1, along with our efforts at achieving the desired JAK1/JAK2 selectivity that allowed identification of a clinical candidate.

RESULTS AND DISCUSSION

Screening strategy: Literature accounts reporting kinase selectivity typically use the ratio of biochemical IC_{50}'s determined at the K_m for ATP. These selectivity ratios are misleading for kinases with dissimilar ATP K_m values and when extrapolating data to cellular settings.[18] JAK1 (K_m = 40 μM) has a K_m for ATP about 10-fold higher than that for JAK2 (4 μM) and JAK3 (4 μM) and about 3-fold higher than that for TYK2 (12 μM). When tofacitinib is assayed at a physiologically relevant concentration of ATP (1 mM), JAK1 and JAK2 potencies are decreased when compared to data obtained at ATP concentrations equal to their respective K_m's. Due to these differences in K_m for ATP, there is a greater potency reduction for JAK2 with its higher affinity for ATP and, as a result, tofacitinib becomes 5-fold more potent for JAK1 than JAK2 at physiological ATP levels. Importantly, the higher potency of tofacitinib inhibition of JAK1 over JAK2 also translates into more potent inhibition of cytokines such as IFNα, which are JAK1-dependent and JAK2-independent, over cytokines such as EPO that are solely JAK2-dependent.[14] Differences in the K_m for ATP may also come into play when assessing selectivity across the kinome as kinases with lower K_m values may appear to have greater activity (biochemical) but may not translate into functional (cellular) assays which are determined at physiologic ATP levels.

When assessing JAK selectivity, the human cytokine inhibition profile in patients is most relevant. However, determination of this required modeling of human whole blood (HWB) potencies onto projected human pharmacokinetics, not a quick and inexpensive analysis to routinely conduct on all project compounds. Clinical data suggested that maximizing JAK1 selectivity over JAK2 in HWB is required to reduce the risk of hematopoietic effects.[16,19] Thus, we routinely generated IC_{50}'s for IFNα stimulation in HWB (JAK1) and CD34+ cells spiked into HWB (JAK2) and measuring the inhibition of phosphorylation of various STATs following

stimulation. These values correlated well with the biochemical enzyme assays conducted at 1 mM ATP.

To identify compounds with a high probability of demonstrating *in vivo* selectivity for JAK1 versus JAK2, we aimed for an *in vitro* selectivity window (biochemical or HWB) of ~25-fold and human liver microsome (HLM) stability of ~8 μL/min/mg or lower for desirable *in vitro* clearance.[20a] These values were chosen to allow for uncertainties in the cellular assays and in the translation of the dynamic range of HLM measurements to *in vivo* clearance. Compounds which met these criteria were selected for advancement into pharmacokinetic and efficacy studies.

Lead analogs – replacing the tofacitinib 3-aminopiperidine group. In our efforts to develop highly selective JAK1 inhibitors, we noted that tofacitinib (**1**) has excellent overall kinome selectivity[15] and attributed much of this beneficial characteristic to the pyrrolopyrimidine hinge-binding motif. Therefore, we opted to retain the pyrrolopyrimidine while a variety of diamine linkers were systematically evaluated as alternatives to the tofacitinib 3-aminopiperidine group. The terminal amino group was capped to obtain a variety of amide and sulfonamide derivatives. As a consequence of this survey, we observed that sulfonamides bearing a *cis*-1,3-cyclobutane diamine linker tended to confer not only excellent potency in the low nanomolar range, but more importantly, excellent selectivity within the JAK family. Interestingly, unlike the 3-aminopiperidine group in **1**, capping the *cis*-1,3-cyclobutane diamine with an amide group resulted in compounds possessing JAK1 activity in the micromolar range (data not shown), significantly less active than the sulfonamide analogs. One of the hits, phenylsulfonamide **4** (Table 1), possessed remarkable potency (JAK1 IC_{50} = 6 nM) and selectivity (69-fold over JAK2) when assayed at an ATP concentration of 1 mM. Although HLM clearance of this compound was high (58 μL/min/mg), we felt that we would be able to improve metabolic

stability by appropriate substitution and reduction of lipophilicity (LogD). The initial cohort of alkyl sulfonamides **5-8** demonstrated increased potency and, importantly, a concomitant increase in JAK1 selectivity as the sulfonamide alkyl group increased in size. Even the simple methanesulfonamide **5** possessed good potency and selectivity for JAK1 (IC_{50} = 90 nM; 14-fold selective over JAK2) suggesting that the sulfonamide series has an inherent potency and selectivity advantage for JAK1. Additionally, the alkyl sulfonamides **5-8** possessed reasonable metabolic stability as measured by HLM. The trifluoroethyl analog **8**, was interesting in that JAK1 potency was ~8-fold higher than the ethyl analog **6**, but selectivity over JAK2 was not improved. Analog **9**, bearing a *p*-fluorophenyl sulfonamide exhibited high JAK1 potency and selectivity versus JAK2 (JAK1 IC_{50} = 3 nM; 80-fold selectivity over JAK2), but unfortunately, like **4**, metabolic stability (39 μL/min/mg) was poor. Potency was somewhat reduced for the benzylsulfonamide **10** (JAK1 IC_{50} = 92 nM) and, like the phenyl sulfonamides, this compound suffered from high HLM (24 μL/min/mg) clearance.

Based on their excellent potency and high selectivity, further optimization efforts focused on the phenylsulfonamides. However, in spite of their impressive activity, extensive modifications to the aryl ring did not result in analogs with acceptable clearance and they were not pursued further (data not shown). All compounds were assessed against JAK3 and TYK2 in a biochemical assay. The majority of the sulfonamide analogs did not possess significant activity for JAK3 (IC_{50}'s ~8 uM to >10 uM) and showed only modest activity against TYK2 (IC_{50}'s >200 nM) (Table S1, Supporting Information).

Analogs **4-10** were evaluated in a HWB assay using IFNα as stimulant to assess JAK1 potency in a cellular system. We also evaluated **5-9** in a HWB assay to which we added $CD34^+$ cells and

used EPO as stimulant to assess JAK2 potency.[14,18] A general observation was made that the HWB potency was right-shifted 5- to 35-fold from the biochemical assay and the shift roughly correlated with LogD of the compounds. In general, we attributed this to plasma protein binding (Figure S2). In addition, the JAK2/JAK1 selectivity ratios in HWB were similar to those derived from the biochemical assays, but with a trend towards being slightly more JAK1-selective. Also potentially contributing to the potency shift was use of the truncated kinase domain in the biochemical assay, whereas in the HWB assay, the full length kinase is present in its native cellular environment at physiologic ATP levels. For these reasons we decided that the HWB assays were most relevant for translating selectivity from *in vitro* to *in vivo*.

With these results and the initial evaluation of sulfonamides **4-10** in hand, it became apparent that smaller, lower LogD compounds would be more likely to possess all of the properties required to advance a molecule to the clinic and we therefore focused our efforts on analogs with smaller alkyl analogs in place of the aryl group in **10.**

[Table 1]

Sulfonamide replacements. Beyond exploration of different sulfonamide derivatives, we also evaluated variants of the sulfonyl-containing linker, namely sulfamides, sulfones and "reverse sulfonamides" (Table 2).

Sulfamide analogs **11-15** possessed smaller alkyl groups and exhibited JAK1 potencies (IC_{50}'s) ranging from 51-144 nM with 8 to 24-fold selectivity over JAK2. The ethyl (**11**), propyl (**12**) and cyclopropyl (**13**) analogs had modest potency but their selectivities were lower, suggesting that shorter alkyl groups in sulfamides do not make efficient interactions with JAK1. Extending the cyclopropyl group by a methylene gave **14**, which improved the JAK1 potency

(IC_{50} = 51 nM) and increased JAK2 selectivity to 21-fold. HLM clearances for **12** and **14** were good, but reduced metabolic stability was noted when larger, more lipophilic alkyl groups were employed to increase potency and selectivity. Thus, analog **15** incorporating a nitrile was prepared to introduce polarity into the alkyl chain and lower LogD. The choice of nitrile as a polar function was based on the reported favorable interaction of the nitrile in **1** with the backbone atoms of the residues of the P-loop i.e. Gly831, Gly834 of JAK3.[20b] However, although **15** exhibited a good metabolic stability and selectivity profile, no enhancement in JAK1 potency was observed.

Sulfones **16-20** (Table 2) exhibited improved JAK1 potencies relative to the sulfamides, however selectivities against JAK2 were not improved. The ethyl analog **16** (JAK1 IC_{50} = 57 nM) was approximately 3-fold more potent than the related sulfamide **11** and about equipotent to the cyclopropyl analog **17**. While an improvement in potency was observed with the *n*-propyl analog **18**, a more significant increase in potency was observed with the longer *n*-butyl analog **19** (IC_{50} = 9 nM), which possessed an improved JAK2 selectivity of 24-fold. This was the first analog to show significant JAK1 selectivity while also having high potency and modest HLM clearance (14 μL/min/mg). We assessed the potency of the sulfones in the HWB assays and, although there was some variability in the right shift, HWB activities were largely in line with biochemical activity. The *n*-butyl analog **19** displayed excellent activity against IFNα (IC_{50} = 155 nM) and good selectivity versus EPO (IC_{50} = 4089 nM). We prepared phenyl analog **20** to assess potency and clearance within an aryl sulfone motif. As previously noted with phenylsulfonamide **4**, the JAK1 potency was exceptional (10 nM), but HLM clearance was high (20 μL/min/mg). Unlike **4**, which showed good selectivity over JAK2 (69-fold), **20** displayed no advantage in terms of selectivity, which was reduced to 16-fold.

The low nanomolar potency previously observed with the sulfonamides and sulfones was again observed with reverse sulfonamides **21-24** (Table 2). For a similar LogD range, the clearance was comparable to the other analogs. However, desirable potency and selectivity levels required introduction of larger alkyl groups as in **23** for which HLM clearance increased from moderate to a high level.

Observations from compounds **4-24** indicated that, for all variants of the sulfonyl-containing linker, selectivity generally improved as the side chains grew larger. Although based on a limited number of examples, the sulfamide subset was of lower interest as these compounds possessed the poorest overall JAK1 potency. A comparison of the JAK1/JAK2 selectivity ratios of sulfonamides to sulfones and reverse sulfonamides suggested that, the sulfonamides were capable of achieving the best selectivities for JAK1: 39-fold for isobutyl analog **7** and 80-fold for *p*-fluorophenyl analog **9**. Selectivity peaked at about 25-fold for the other series containing similar alkyl and aryl groups. We also observed a trend that suggested HLM clearance values were often >8.0 μL/min/mg when $LogD_{7.4}$ exceeded 2.0. Based on these observations, the alkyl sulfonamide series appeared to provide the best balance of potency and clearance. We thus prepared an additional cohort of alkyl sulfonamides (Table 3).

In order to determine the impact of stereochemistry on potency and selectivity, the 1,3-*trans*-cyclobutyl analog of **25** was prepared and evaluated. Whereas the *cis*-configured isomer **25** showed good potency (JAK1 IC_{50} = 29 nM), the *trans* isomer **26** suffered a ~20-fold loss in potency. Since the JAK2 IC_{50} of **26** was greater than that of the top screening concentration, we were unable to determine its JAK2/JAK1 selectivity ratio.

The addition of a methyl to give linear (**27**) butyl chain resulted in a ~3-fold increase in potency relative to **25**, the expected increase for a non-specific hydrophobic interaction of methyl with a protein.[21] However, this addition increased LogD to 2.4, resulting in a concomitant increase in HLM clearance to 17 μL/min/mg. The incorporation of cyclopropyl rings as in **28** and **29** did not afford an improvement in potency or selectivity over the simple linear analogs **25** and **27**, but the reduced LogD of the cyclopropyl group did improve HLM clearance. In contrast, cyclobutylmethyl analog **30**, which did not afford a reduction in LogD, demonstrated improved potency and selectivity, but displayed higher clearance. The incorporation of trifluoromethyl within the side chain to improve metabolic stability was successful as analogs **31** and **32** maintained JAK1 potency and low clearance (<8.0 μL/min/mg) while displaying increased selectivity (54-fold and 61-fold respectively). The ether analogs **33** and **34** were weaker in potency, but retained low clearance when compared to the trifluoromethyl analogs.

In the HWB assays, the simple alkyl analogs **25-30** had potency shifts compared to the biochemical assay similar to the earlier sulfonamide cohort, while the groups containing heteroatoms **31-34** appeared to have greater right shifts than would be expected based on LogD alone. For example, compound **31**, which has a similar LogD value and JAK1 biochemical potency comparable to **30**, shows a larger right shift (63 vs. 20 fold for **30**) in the HWB IFNα assay. The right shift in the HWB CD34+ EPO assay was more variable, but generally agreed with the magnitude of the right shift observed in the IFNα assay.

At this stage we were pleased that several compounds, especially sulfonamides **25**, **28**, and **29**, exhibited promising overall profiles including good JAK1 potency (biochemical and HWB INFα $IC_{50} \leq 0.05$ μM and ≤ 0.3 μM respectively), good JAK1/JAK2 selectivity (≥ 25-fold), and high *in*

vitro metabolic stability (HLM ≤ 9 μL/min/mg). Although HLM clearance for sulfone **19** was somewhat higher (~14 μL/min/mg), its profile was also attractive in terms of potency (JAK1 IC_{50} = 9 nM) and selectivity (24-fold). Comparing sulfonamides **25**, **28**, and **29**, compound **25** was the most selective based on ratios determined using HWB IC_{50}s (38-fold vs. 22- and 29-fold for **28** and **29**, respectively). Thus, representing two structural series (sulfones and sulfonamides), compounds **19** and **25** were selected for further profiling from among the analogs shown in Tables 1-3 (*vide infra*).

[Table 3]

X-ray crystallographic studies – understanding JAK1/JAK2 selectivity. While initial compound synthesis and evaluation was in progress, we developed a robust crystallographic soaking method enabling the routine determination of JAK1 inhibitor structures.[22] Notably, we determined the X-ray structure of compound **25** in complex with the kinase domains of JAK1 (2.1 Å) and JAK2 (1.8 Å). This effort built upon our knowledge of these important tyrosine kinases and provided invaluable insight into the observed JAK1/JAK2 selectivity (28-fold) of compound **25**.

The overall folds of the two kinase domains are similar to those previously reported[23] (R.M.S.D ~0.80 Å. Although the JAK1 kinase domain shares only 53% overall sequence identity with JAK2, most of the residues in the ATP-binding site are conserved between the two enzymes. The residue differences (within 5 Å radius from the ligand) are located in the hinge region, phosphate-binding region, i.e., P-loop (Table 4) and in the solvent exposed regions towards the periphery of the binding site. While at first these differences may seem sufficient for a ligand to achieve a high level of selectivity, these residues point away from the ligand, and

hence they are not amenable for direct hydrogen bonding contacts with the ligand. There is one exception, the Glu966(JAK1)/Asp939(JAK2) residue difference that lies towards the solvent-exposed region of the binding site (Figures 2 and 3). This difference has been specifically targeted in the literature for a differential hydrogen bonding interaction with favorable improvement in JAK1 selectivity (36 fold).[24] This observation was supported by co-crystal structures of both JAK1 and JAK2 that indeed revealed differential interaction between the two isoforms. Additionally, Vasbinder and coworkers observed water-mediated hydrogen bonds between Glu966 and a potent JAK1-selective inhibitor.[25]

[Table 4]

Comparison of the crystal structures of **25** bound to both JAK1 and JAK2 showed that, although the ligand binding mode is similar in both cases, there are subtle differences in hydrogen bonding pattern with residues within the binding site and in the orientation of the propyl tail group in the P-loop region that could contribute to the JAK1 selectivity. The core pyrrolopyrimidine ring of the ligand in both structures makes two critical hinge binding interactions, the pyrrole NH with the carbonyl backbone of Glu957(JAK1)/Glu930(JAK2) and the pyrimidine N1 nitrogen with the NH backbone of Leu959(JAK1)/Leu932(JAK2) residues.

There are other differences in the structures that we believe contribute to overall ligand selectivity, for example a water molecule is in position to bridge a hydrogen bond interaction between the N3 of the pyrimidine ring and the side chain Glu966 residue in JAK1. In JAK2, due to the shorter Asp939 residue at this position, a direct water mediated bridge interaction is not possible and requires an extended network of water molecules in the solvent-exposed region to make interaction with the N3 atom. Although the extent to which this differential interaction

contributes to selectivity is difficult to predict, these differences in the hydrogen bonding pattern could have influence on the JAK1 selectivity of **25**.

[Figures 2 and 3]

In both structures, the observed conformation of the sulfonamide group has the H-N-S-O dihedral at 1-10°. A search of this fragment in the Cambridge Crystallographic Database[26,27] indicated that this is a preferred conformation for this group. It is believed that this conformation allows the nitrogen lone pair to favorably interact with the sulfur d-orbitals. The *cis* configuration of the puckered cyclobutyl ring allows the NH of the sulfonamide to be in a position to pick up hydrogen bond interactions with both the backbone carbonyl of Arg1007(JAK1)/Arg980(JAK2) and also the side chain of Asn1008(JAK1) /Asn981(JAK2) in both structures. We did observe differences in the rotamer states of the Arg residue, for example, in the JAK2 X-ray structure, a single rotamer was observed for the Arg980 residue which allows a hydrogen bond from the side chain of Arg980 to the SO_2 group of the ligand. In JAK1, this particular rotamer is only observed as a minor state. Additionally in JAK2, there is a water mediated hydrogen bond observed between oxygen of the SO_2 group and NH backbone of the Lys857 residue in the P-loop which could influence the flexibility of the P-loop. This will be discussed in detail in the next section.

A difference in the orientation of the *n*-propyl group of the ligand towards the P-loop region was observed when comparing the two JAK structures. In both structures the electron densities of the P-loop and ligand were well resolved, which aided general conclusions on the origin of ligand selectivity from this region. A comparison of the crystal structures of **25** bound to JAK1 and JAK2 (Figure 4) suggested that the P-loop in JAK2 is clamped down slightly more onto the

active site than the one observed in the relatively more open JAK1 P-loop. It is possible that although the side chains of residues within the P-loop region are oriented away from the ligand binding site, the residue differences between the JAK1 and JAK2 (Table 4) along the P-loop may still affect the rigidity of the P-loop and allow different conformations to be accessed by JAK1 compared to JAK2. A shift in the P-loop position observed between the JAK1 and JAK2 X-ray structures has been previously invoked to explain the selectivity of a series of imidazopyrrolopyridines.[28]

[Figure 4]

As a consequence of the disparate P-loop orientations, the ligand is forced to adopt different conformations in the bound states for the two torsion angles, i.e., $S(O_2)$-C-C-C and N-$S(O_2)$-C-C, in order to maximize its shape and electrostatic complimentarity with the P-loop. To get a better understanding of the energetics associated with these dihedrals, we calculated the torsion profile using the simple fragment *N*-methylpropane-1-sulfonamide in a quantum mechanical calculation at B3LYP/6-31++G level[29] (Figures 5a and 5b). For both dihedrals, two minima are observed, i.e., anti and gauche, with the anti being lower in energy. In the JAK1 structure, the ligand adopts a low energy anti conformation for the propyl chain, i.e., $S(O_2)$-C-C-C dihedral ~175°, while in JAK2 a higher energy (ΔE = 1.2 kcal/mol) conformation exists having a dihedral of ~95°. In contrast, the observed torsional angle N-$S(O_2)$-C-C is in a high energy (ΔE = 3.2 kcal/mol) conformation in JAK1 (dihedral of 126°), while a lower energy dihedral (171°) is seen in JAK2. These calculations suggest that, in both ligand bound states, an internal energy penalty is paid by the ligand to adopt a conformation that makes efficient van der Waals and electrostatic interactions with the P-loop. While the overall energy penalty is calculated to be higher in JAK1,

the ligand seems able to overcome the conformational penalty from the N-S(O_2)-C-C torsion by forming more favorable van der Waals contacts with the P-loop, thus improving JAK1 selectivity. This is consistent with the observed trend of increase in selectivity with larger alky groups as these are able to make better P-loop interactions in JAK1 than JAK2, i.e., **5** (14-fold), **6** (>19-fold), **25** (28-fold) and **27** (66-fold).

[Figure 5a and 5b]

Structure-enlightened "second generation" analog design

Based on insights provided from the X-ray crystallography studies and analysis, a number of new analogs were prepared in the sulfamide, sulfonamide and reverse sulfonamide series (Table 5).

[Table 5]

Sulfamides: As noted previously, the observed conformation of sulfonamide **25** has an H-N-S-O dihedral[30] of ~10°, which allows for the stabilization of this rotamer by the nitrogen lone pair interaction with the sulfur d orbitals. We reasoned that, in the case of sulfamides, the distal NH (i.e., NH furthest from the pyrrolopyrimidine ring) would form a similar interaction with the other S=O group, giving rise to an s-*cis*, s-*trans* conformation (Figure 6a). Indeed, a search of the Cambridge Crystallographic Database for acyclic sulfamides revealed a strong preference for this conformation. All 21 CSD entries from the search displayed a preference for the s-*cis*, s-*trans* conformation (for example, see Figure 6b). Interestingly, this conformational preference implies that, in the bound state, the ligand would favor the proximal NH in an s-*cis* configuration so as to make hydrogen bond interactions with both the backbone carbonyl of

Arg1007(JAK1)/Arg980(JAK2) and the side chain of Asn1008(JAK1) /Asn981(JAK2), while the distal NH would be favored in an *s-trans* conformation. This would have the undesirable effect of orienting the R-group away from the P-loop and thus have a detrimental effect on JAK1 potency. We reasoned that this was a possible explanation for the lower potency and selectivity observed with the sulfamides **11-15.** We hypothesized that *N*-alkylation of the distal sulfamide nitrogen would disrupt the conformational preference of the distal N-H-S-O group and thereby allow the R-group to make an interaction with the P-loop and potentially improve potency. Indeed, *N*-methyl analogs **37** and **38** exhibited a 4 to 7-fold increase in potency for JAK1 over the non-methylated analogs **11** and **13** respectively and >2-fold increase in JAK1/JAK2 selectivity (Table 5). This was attributed to the asymmetric nature of the substituents on the distal nitrogen that allows the alkyl group, i.e., ethyl in **37** and cyclopropyl in **38**, to be directed towards the P-loop. We also prepared symmetrical piperidine **39**, which retained JAK1 potency and demonstrated improved JAK2/JAK1 selectivity. Unfortunately, **37** and **38** still lacked the desired selectivity, while **39** had poor HWB potency and HLM stability. Thus, in spite of the improvements in potency and selectivity, the overall profiles were not improved.

Based on the mixed results seen with these "second generation" sulfamides, no further advancement of the compounds was undertaken and we focussed our efforts on the sulfonamide and reverse sulfonamide analogs.

[Figure 6a and 6b]

Sulfonamides: Applying insight from our structural studies indicating that the sulfonamide NH group is an important determinant of JAK1 selectivity and that interaction of the alkyl group with the P-loop contributes to potency and selectivity, sulfonamides containing polar

functionality were prepared (Table 5). The choice of polar groups was based on the reported interaction of nitrile in **1** with the P-loop of JAK3 to confer high potency. Compound **35** containing the nitrile functionality was potent, metabolically stable and had excellent selectivity. Its potency in the HWB IFNα assay **(**IC_{50} = 216 nM) was in a desirable range and was well separated from HWB EPO (IC_{50} >6934 nM). The oxetane **36** had a similar profile, demonstrating excellent potency and selectivity in the HWB assays and high metabolic stability. Although only slightly more potent than the acyclic ether **34** in the JAK1 biochemical assay, the LogD was reduced by 0.5 which may account in part for the 4-fold improvement in HWB IFNα potency.

Reverse Sulfonamides: Based on the success with distal *N*-methylation in the sulfamide series, we prepared additional *N*-methyl reverse sulfonamides having the potential for improvements in potency and selectivity through interactions with the P-loop. Analogs **41** and **42** (Table 5) showed the expected improvements in JAK1 potency and selectivity versus JAK2 when compared to the corresponding NH analogs **23** and **24**. These results are comparable in magnitude to those observed with the sulfamides. Cyclopropylmethyl analog **42** demonstrated good HWB IFNα potency, but suffered from poor metabolic stability. Once again we introduced symmetry to improve selectivity and prepared the pyrrolidine sulfonamide **43** as a cyclized version of *n*-butyl sulonamide **23**. The potency was modestly improved, but selectivity was reduced, likely due to the smaller size of the unsubstituted 5-membered ring and resulting weaker interaction with the P-loop. In this cohort, high selectivity was associated with poor metabolic stability although HWB activity was acceptable for several analogs.

Pharmacokinetics. Based on JAK1 potency (biochemical and HWB), JAK1/JAK2 selectivity, and acceptable *in vitro* metabolic stability, "second generation" sulfonamides **35** and **36** (Table

5) were selected for pharmacokinetic profiling along with sulfone **19** (Table 2) and sulfonamide **25** (Table 3). Pharmacokinetic parameters were determined in rat at 1 mg/kg i.v. or 3 mg/kg p.o. (Table 6). Clearances of **19** and **25** were low relative to total liver blood flow, whereas **35** and **36** showed higher clearance values. Oral bioavailability was better for compounds **19** and **25**, consistent with lower clearance as well as good *in vitro* permeability and solubility. In addition, volumes of distribution were moderate (0.74-1.99 L/kg) for this cohort of analogs. Accordingly single species allometric scaling predicted more favorable human clearance values for compounds **19** and **25** compared with **35** and **36**.

[Table 6. PK properties in the S-D rat following doses of 1 mg/kg i.v. or 3 mg/kg p.o. and in vitro physicochemical properties]

Although compounds **19** and **25** showed similar pharmacokinetic profiles and similar potencies in JAK biochemical and cellular assays, a broad functional CEREP screen at 10 μM consisting of a diverse set of GPCR, ion channel, transporter and enzyme (64 targets in total) for off-target effects indicated that **19** showed activity against the CB-1 receptor in a binding assay (IC_{50} = 120 nM). This translated into observed motor effects consistent with CB-1 inhibition in a rat toxicokinetic study. Compound **25** showed no measurable activity (>50%) at any targets profiled with the exception of KDR kinase (VEGFR2, IC_{50} = 1.2 μM) and weak activity on monoamine oxidase A (MAO-O, IC_{50} = 6 μM). A follow-up study in a functional Caliper whole cell KDR kinase assay showed no effects on KDR kinase activity at concentrations up to 30 μM.

Sulfonamide **25** was also evaluated in a broad kinase panel (Table S3), which indicated that it is a highly selective compound, crossing over most potently onto JAK3 with 61% inhibition at 1 uM. The lack of off-target kinase inhibition is particularly notable, given that the broad kinase

panel was run at the K_m of ATP to maximize assay sensitivity for the detection of potential off-target activity. Although JAK3 showed up as an off-target in the broad kinase panel, **25** had an IC_{50} of 605 nM when measured at the K_m of ATP and >10 μM when measured at 1 mM ATP. In summary, compound **25** is a potent JAK1 inhibitor with 28-fold selectivity over JAK2, >340-fold over JAK3 and 43-fold over TYK2 (Table S1) at 1mM ATP and an excellent selectivity profile over the broader kinome. Based on its favorable overall properties and pharmacokinetic profile across multiple species (Tables S4 and S5), **25** progressed into pharmacodynamic and efficacy studies *in vivo*.

Rat Target Modulation. The *in vivo* pharmacokinetic-pharmacodynamic relationship of **25** was characterized following single oral doses of 5, 15, and 50 mg/kg to naïve Lewis rats. Serial blood samples were taken at 0.25, 0.5, 2, 4, 8, and 24 hours and analyzed for drug concentrations and STAT phosphorylation (pSTAT) activities. pSTAT1 was measured following *ex vivo* stimulation of blood with IL-6 or IFNγ to assess JAK1/JAK2 signal inhibition, while pSTAT3 was measured following stimulation with IL-21 to assess JAK1/JAK3 signal inhibition (Figure 7). The inhibition of pSTAT formation induced by IFNγ, IL-21 and IL-6 was directly linked to the plasma concentration of **25** and was independent of time. The respective calculated unbound plasma IC_{50} values were 191, 938 and 176 nM.

[Figure 7 Target Modulation plots]

Rat adjuvant-induced arthritis model. The effect of JAK1 inhibition by **25** *in vivo* was evaluated using a therapeutic dosing paradigm in a rat adjuvant-induced arthritis (AIA) disease model[31a]. Female Lewis rats immunized with complete Freund's adjuvant were dosed orally with **25** or vehicle for seven consecutive days after disease onset as measured by hind paw volume

using plethysmography. Paw volumes and weights were followed throughout the study. At the end of seven days of dosing, plasma concentrations of **25** were assessed. Two studies were completed. In the initial study, immunized rats were dosed QD with either: 5, 15, or 50 mg/kg of **25** or vehicle (PO) (Figure S3). Since a significant reduction in paw swelling was observed for all doses, a second study was conducted focused on lower doses (0.5, 1, 5, or 15 mg/kg **25** or vehicle control) were evaluated. A significant reduction of hind paw swelling was observed down to 1 mg/kg (Figure 8, Days 6-7). Collective pharmacodynamics modeling of both studies using an E_{max} model fit indicated an unbound $Cave_{50}$ of approximately 1.3 μM ($r^2 \sim 0.91$) (Figure 9).

[Figure 8 Disease activity plots]

[Figure 9 Emax modeling Cave]

To determine the effect of **25** on JAK2/JAK2 dependent GM-CSF signaling, blood samples were taken at peak plasma concentration (0.25 hr post dose) in the rats treated with **25** on day 7. GM-CSF induced pSTAT5 in monocytes was reduced by approximately 30% at the top dose of 15 mg/kg and less than 5% at lower doses. In contrast, IL-21, IFNα and IFNγ induced stat phosphorylation was reduced >60% at 1 mg/kg.

Human prediction of pharmacokinetics and pharmacodynamics. The primary clearance mechanisms of compound **25** were determined to be mediated by CYP450 metabolism, with

limited renal and biliary clearance expected. Human clearance predictions were made using human liver microsomes and hepatocyte data as well as standard single species allometric scaling techniques, all of which suggested low to moderate human clearance would be observed (Table 7).

[Table 7]

Preclinical and clinical studies with JAK inhibitors have shown the value in using average drug plasma concentration (Cave) in predicting anti-inflammatory response.[19,31b,32] The percent level of cytokine inhibition (IC_{xx}) of compound **25** for each cytokine pathway can be calculated by combining the corresponding unbound whole cell IC_{50} value (Table 8) with the predicted unbound human Cave value (i.e., $IC_{xx} = 100*Cave/(IC_{50} + Cave)$). The overall selectivity profile of cytokine inhibition can be visualized at an expected efficacious human dose of 200 mg QD (based on human hepatocyte scaling), which is expected to achieve a $Cave_{80}$ for IFNα using this method of analysis (Figure 10). Selectivity of inhibition of compound **25** for cytokines signaling through JAK1 heterodimer pairs (IFNα, IFNγ, IL-6, IL-10, IL-15, IL-21, IL-23 and IL-27) (Table 8) was evident compared to the sparing of JAK2/JAK2 (EPO) and JAK2/TYK2 (IL-12 and IL-23) signaling. Additional data showing the cytokine inhibition profile for compounds **19, 35, 36** in the HWB assays is shown in Table S6.

[Table 8]

CHEMISTRY

Preparative routes to the sulfonamide and sulfamide analogs are shown in Scheme 1.

Benzyl (3-oxocyclobutyl)carbamate (**44**) was condensed with methylamine (AcOH/THF/rt) and then treated with $NaBH_4$ (0°C to rt) to afford cyclobutylamine **45** as a mixture of *cis* and *trans* isomers. Hydrochloride salt formation followed by recrystallization allowed the isolation of the major isomer, *cis*-**45**·HCl, in moderate yield (63%). In addition the minor isomer *trans*-**45** (used for the preparation of **26**), could be isolated by supercritical fluid chromatography. Subsequent reaction of *cis*-**45**·HCl with 4-chloro-7-[(4-methylphenyl)sulfonyl]-7*H*-pyrrolo[2,3-*d*]pyrimidine (**46a**)[33] in presence of DIPEA (*i*-PrOH/75°C) provided the protected intermediate **47a**. Here, the electron-withdrawing tosyl protecting group allowed the nucleophilic aromatic substitution reaction to occur readily in high yield (95%).

[Scheme 1]

Treatment of **47a** with HBr (EtOAc/AcOH/rt) served to remove the pendant carbobenzyloxy protecting group and provided **48a**, isolated as the stable, free-flowing dihydrobromide salt. Conversion of **48a**·2HBr to target sulfonamides was then achieved in two steps: sulfonylation (RSO_2Cl/ base) followed by removal of the tosyl group. Typically aqueous hydroxide was used for the deprotection step, but occasionally, due to the potential for side reactions involving the sulfonamide side-chain, other conditions were used such as in the preparation of **35**, where the presence of the nitrile function necessitated use of Cs_2CO_3 as base.

Several sulfonamide analogs were prepared starting with 2,4-dichloro-7*H*-pyrrolo(2,3-*d*)pyrimidine (**46b**). Though less robust, this route was generally useful in compound preparation, not requiring the sometimes problematic tosyl deprotection step. Taking advantage of the activation effect of the additional chlorine atom on the pyrrolopyrimidine ring, **46b** was combined with *cis*-**45**·HCl (K_2CO_3/H_2O/95°C) to afford adduct **47b** in high yield (98%).

Exposure of **47b** to catalytic hydrogenation conditions ($Pd(OH)_2$) then gave amine **48b**, which was taken on either as the hydrochloride salt or as the free base.

Sulfonamide formation using **48b** could be carried out directly under standard conditions (RSO_2Cl/base) but often mixtures arose and yields were low due to competing sulfonylation of the pyrrolopyrimidine NH. This problem could be avoided by *in situ* protection of the pyrrolopyrimidine NH function. Thus **48b** (hydrochloride) was first treated with LiHDMS (2.2.eq.) and TMSCl (2.2 eq.) in THF to provide what was assumed to be a bis-TMS derivative (pyrrolidine NH and primary amine capped by TMS). Addition of RSO_2Cl then afforded the desired sulfonamide target after workup, presumably via preferential sulfonylation of –NHTMS.

As shown in Scheme 1, sulfamide analogs were accessed via reaction of *N*-sulfamoyloxazolidinone **50**, prepared from **48a**·2HBr by the method of Montero[34] with primary and secondary amines (R^1R^2NH) at elevated temperature in the presence of base (TEA or DIPEA).[35] As with the preparation of sulfonamides, removal of the *N*-tosyl group was typically carried out using aqueous LiOH or NaOH, often in the presence of a co-solvent such as EtOH.

Compounds in the reverse sulfonamide and sulfone series were prepared starting with the two step conversion of ethyl 3-aminocyclobutanecarboxylate hydrochloride (*cis*/*trans* = 10:1) (**52**·HCl)[36] to 3-(methylamino)cyclobutyl]methanol (**53**), also a 10:1 mixture of *cis*- and *trans*-isomers (Scheme 2). Reaction of **53** with 4-chloro-7-[(4-methylphenyl)sulfonyl]-7*H*-pyrrolo[2,3-*d*]pyrimidine (**46a**) (TEA/KI/acetone/56°C) gave alcohol **54** as a mixture of isomers (85%) which were separated by supercritical fluid chromatography. The major isomer, *cis*-**54** was then advanced in good overall yields to common intermediates **55a** and **55b** via *O*-tosylation and *O*-

mesylation respectively (*p*-TsCl or MsCl/DMAP/DCM). Tosylate displacement on **55a** with potassium thioacetate (DMF/55°C) provided *S*-acetate **56**.

[Scheme 2]

Compounds in the reverse sulfonamide series (Scheme 2) were obtained in four steps from **56**. Oxidation to sulfonic acid **57a** (aq. H_2O_2/HCO_2H) followed by reaction with thionyl chloride (cat. DMF/DCM/0°C) provided sulfonyl chloride **57b** which, after sulfonamide formation (R^3R^4NH/base) and deprotection, gave the target analogs.

Sulfone analogs could be accessed in two or three steps from either tosylate **55a** or mesylate **55b**. Sulfonate displacement with *in situ* generated thiolate (R^2SH/DBU/NMP/rt) provided thioethers of general structure **58a**, which usually underwent cleavage of the *N*-tosyl group under the reaction conditions to afford deprotected thioethers **58b**. In some cases, tosyl cleavage was incomplete, necessitating a subsequent tosyl group removal step (e.g., aq. LiOH/EtOH). Oxidation of **58b** with Oxone® then provided the target sulfones. These could also be prepared via *S*-acetate **56** starting with cleavage of the acetyl group ($K_2CO_3/NaBH_4$/MeOH/0°C)[38] and *in situ* alkylation of the resulting thiolates with alkyl halides, alkyl tosylates and alkyl mesylates (R^2-X). The product thioethers **58a** then afforded the target sulfone analogs after tosyl group cleavage and oxidation. Sulfone synthesis via **56** became a preferred method as it obviated the need to use thiols as starting materials.

CONCLUSION

By replacement of the 3-aminopiperidine in tofacitinib (**1**) with a *cis*-1,3-cyclobutyldiamine capped with a sulfonamide, we were able to identify highly potent and selective JAK1 inhibitors in good physicochemical space. We found that various permutations around the sulfonyl moeity (i.e., sulfamides, sulfones and reverse sulfonamides) also afforded potent and selective molecules. Clearance was recognized as a key factor in identifying compounds suitable for development. Therefore the observation that compounds with LogD < 2 demonstrated very low HLM clearance enabled us to design molecules with the right balance of lipophilicity and polarity required for good potency and metabolic stability. Profiling in HWB assays demonstrated that the excellent potency for JAK1 translated to a cellular system and that JAK2 selectivity, as assessed by the inhibition of EPO in $CD34^+$ cells was confirmed relative to the biochemical assays. Insights obtained through X-ray crystallography as to how analogs bind to JAK1 allowed us to improve potency, especially within the sulfamide and reverse sulfonamide series. Assessment of rat pharmacokinetics for the four analogs that met advancement criteria demonstrated that two (**19** and **25**) had low *in vivo* clearance values. Compound **25** exhibited a superior pharmacology profile compared to **19** and therefore was further advanced. Compound **25** was 28-fold selective over JAK2, >340-fold over JAK3 and 43-fold over TYK2 at 1 mM ATP and demonstrated broad kinase selectivity. In a rat target modulation study, compound **25** inhibited pSTAT formation induced by IL-6, IL-2 and IFNγ in a manner directly linked to the drug plasma concentration. Similarly, compound **25** demonstrated efficacy in a dose-responsive manner in a therapeutic rat AIA model. By using allometric scaling and human hepatocyte clearance a human dose of approximately 200 mg QD was projected to achieve $Cave_{80}$ inhibition of IFNα. Following appropriate *in vivo* toxicological testing, compound **25** (PF-04965842)[37] progressed into a Phase 1 clinical study, the results of which will be reported elsewhere.

EXPERIMENTAL SECTION

Chemistry – general information. Chemicals were typically obtained from Sigma-Aldrich or Alfa Aesar and used as received, unless noted otherwise. Solvents were commercial anhydrous grade, used as received. Unless otherwise stated, reactions were run under a positive pressure of nitrogen at ambient temperature. Except where otherwise noted, "chromatographed" and "flash chromatography" refer to normal phase chromatography using a medium pressure Biotage or ISCO system employing commercial pre-packed silica gel columns. Supercritical fluid chromatography (SFC) was performed on an Agilent SFC system in APCI negative mode. Analytical thin layer chromatography (TLC) was performed on 60 Å F254 glass plates pre-coated with a 0.25-mm thickness of silica gel purchased from EMD Chemicals Inc. TLC plates were visualized with UV light. Except where otherwise noted, purities of compounds used in biological studies were >95%, determined by HPLC, UPLC or LC/MS. Ultraviolet (typically 215-220 nm) and evaporative light scattering detection (ELSD) were typically employed for detection.

Nuclear magnetic resonance (^{1}H NMR) spectra were recorded on a Bruker or Varian spectrometer operating at 400 MHz, or a Bruker spectrometer operating at 500 MHz. Chemical shifts are reported in parts per million (δ) relative to $CDCl_3$ (7.26 ppm), DMSO-d_6 (2.50 ppm), MeOH-d_4 (3.31 ppm) or D_2O (4.79 ppm). The following abbreviations are used for peak multiplicites: s = singlet, d = doublet, t = triplet, q = quartet, m = multiplet, br = broadened, dd = doublet of doublets, dt = doublet of triplets.

Low resolution mass spectroscopy was carried out using liquid chromatography−mass spectrometry (LC/MS) on a Waters Acquity UPLC instrument using atmospheric pressure chemical ionization (APCI) or electrospray ionization (ESI).

***N*-(*cis*-3-(Methyl(7*H*-pyrrolo[2,3-*d*]pyrimidin-4-yl)amino)cyclobutyl)benzenesulfonamide (4).** This sulfonamide analog was prepared using a procedure similar to that used to prepare compound **25** starting from **48a**·HBr. ^{1}H NMR (400 MHz, DMSO-d_6): 12.42 (br s, 1H), 8.27 (s, 1H), 8.08 (d, J = 9.0 Hz, 1H), 7.85 (d, J = 7.0 Hz, 2H), 7.55-7.74 (m, 3H), 7.30-7.42 (m, 1H), 6.75-6.92 (m, 1H), 4.58-4.82 (m, 1H), 3.46-3.73 (m, 1H), 3.26 (s, 3H), 2.28-2.46 (m, 2H), 1.95-2.18 (m, 2H). LC/MS m/z (M + H^+) calcd for $C_{17}H_{20}N_5O_2S$: 358. Found: 358.

***N*-{*cis*-3-[Methyl(7*H*-pyrrolo[2,3-*d*]pyrimidin-4-yl)amino]cyclobutyl}methanesulfonamide (5).** This sulfonamide analog was prepared using a procedure similar to that used to prepare compound **25** starting from **48a**·HBr. ^{1}H NMR (DMSO-d$_6$, 400 MHz): 11.64 (br s, 1H), 8.10 (s, 1H), 7.40 (d, J = 8.8 Hz, 1H), 7.14-7.16 (m, 1H), 6.63-6.64 (m, 1H), 4.90-4.98 (m, 1H), 3.54-3.64 (m, 1H), 3.25 (s, 3H), 2.89 (s, 3H), 2.58-2.65 (m, 2H), 2.20-2.28 (m, 2H). LC/MS m/z (M + H^+) calcd for $C_{12}H_{18}N_5O_2S$: 296. Found: 296.

***N*-{*cis*-3-[Methyl(7*H*-pyrrolo[2,3-*d*]pyrimidin-4-yl)amino]cyclobutyl}ethanesulfonamide (6).** This sulfonamide analog was prepared using a procedure similar to that used to prepare compound **25** starting from **48a**·HBr. ^{1}H NMR (DMSO-d$_6$, 400 MHz): 11.64 (br s, 1H), 8.10 (s, 1H), 7.50 (d, J = 8.5 Hz, 1H), 7.15-7.16 (m, 1H), 6.63-6.65 (m, 1H), 4.87-4.94 (m, 1H), 3.53-3.61 (m, 1H), 3.26 (s, 3H), 2.97 (q, J = 7.7 Hz, 2H), 2.57-2.62 (m, 2H), 2.21-2.27 (m, 2H), 1.21 (t, J = 7.7 Hz, 3H). LC/MS m/z (M + H^+) calcd for $C_{13}H_{20}N_5O_2S$: 310. Found: 310. Purity (HPLC) = 98.5% (UV), 85.7% (ELSD).

2-Methyl-*N*-{*cis*-3-[methyl(7*H*-pyrrolo[2,3-*d*]pyrimidin-4-yl)amino]cyclobutyl}propane-1-sulfonamide (7). This sulfonamide analog was prepared using a procedure similar to that used to prepare compound **36** starting from **48b**·HCl. White solid, 52% yield. ^{1}H NMR (400 MHz, DMSO-d_6): 11.62 (br s, 1H), 8.10 (s, 1H), 7.49 (d, J = 9.4 Hz, 1H), 7.13-7.15 (m, 1H), 6.65 (dd, J = 2.0, 3.5 Hz, 1H), 4.85-4.94 (m, 1H), 3.52-3.63 (m, 1H), 3.24 (s, 3H), 2.85 (d, J = 6.6 Hz, 2H), 2.56-2.62 (m, 2H), 2.18-2.26 (m, 2H), 2.04-2.14 (m, 1H), 1.02 (d, J = 7.0 Hz, 6H). LC/MS m/z (M + H$^+$) calcd for $C_{15}H_{24}N_5O_2S$: 338. Found: 338. Anal. calcd for $C_{15}H_{23}N_5O_2S$: C, 53.39; H, 6.87; N, 20.75; S, 9.50. Found: C, 53.27; H, 7.13; N, 20.58; S, 9.12.

2,2,2-Trifluoro-*N*-{*cis*-3-[methyl(7*H*-pyrrolo[2,3-*d*]pyrimidin-4-yl)amino]cyclobutyl}ethanesulfonamide (8). This sulfonamide analog was prepared using a procedure similar to that used to prepare compound **36** starting from **48b**·HCl. White solid, 65% yield. ^{1}H NMR (400 MHz, DMSO-d_6): 11.63 (br s, 1H), 8.22 (d, J = 8.8 Hz, 1H), 8.10 (s, 1H), 7.15 (d, J = 2.5, 3.5 Hz, 1H), 6.62 (dd, J = 2.0, 3.5 Hz, 1H), 4.85-4.94 (m, 1H), 4.36 (q, J = 10.0 Hz, 2H), 3.62-3.72 (m, 1H), 3.25 (s, 3H), 2.59-2.66 (m, 2H), 2.22-2.30 (m, 2H). LC/MS m/z (M + H$^+$) calcd for $C_{13}H_{17}F_3N_5O_2S$: 364. Found: 364. Anal. calcd for $C_{13}H_{16}F_3N_5O_2S$: C, 42.97; H, 4.44; F, 15.69; N, 19.27; S, 8.82. Found: C, 42.64; H, 4.23; F, 15.89; N, 19.08; S, 9.75.

4-Fluoro-*N*-(*cis*-3-(methyl(7*H*-pyrrolo[2,3-*d*]pyrimidin-4-yl)amino)cyclobutyl)benzenesulfonamide (9). This sulfonamide analog was prepared using a procedure similar to that used to prepare compound **25** starting from **48a**·HBr. ^{1}H NMR (400 MHz, DMSO-d_6): 12.44 (br s, 1H), 8.27 (s, 1H), 8.11 (d, J = 9.0 Hz, 1H), 7.82-7.93 (m, 2H), 7.39-7.50 (m, 2H), 7.32-7.39 (m, 1H), 6.85 (d, J = 2.0 Hz, 1H), 4.69 (m, 1H), 3.57 (m, 1H), 3.25 (s, 3H), 2.30-2.44 (m, 2H), 2.00-2.16 (m, 2H). LC/MS m/z (M + H$^+$) calcd for $C_{17}H_{19}FN_5O_2S$: 376. Found: 376.

***N*-(*cis*-3-(Methyl(7*H*-pyrrolo[2,3-*d*]pyrimidin-4-yl)amino)cyclobutyl)-1-phenylmethanesulfonamide (10).** This sulfonamide analog was prepared using a procedure similar to that used to prepare compound **25** starting from **48a**·HBr. ^{1}H NMR (400 MHz, DMSO-d_6): 12.46 (br s, 1H), 8.31 (s, 1H), 7.59 (d, J = 8.6 Hz, 1H), 7.27-7.48 (m, 6H), 6.78-6.97 (m, 1H), 4.72 (m, 1H), 4.31 (s, 2H), 3.47-3.71 (m, 1H), 3.32 (s, 3H), 2.57-2.75 (m, 2H), 2.13-2.41 (m, 2H). LC/MS m/z (M + H$^+$) calcd for $C_{18}H_{22}N_5O_2S$: 372. Found: 372.

***N*-Ethyl-*N*'-{*cis*-3-[methyl(7*H*-pyrrolo[2,3-*d*]pyrimidin-4-yl)amino]cyclobutyl}sulfamide (11).** This sulfamide analog was prepared using a procedure similar to that used to prepare compound **14**, starting with intermediate **50**. ^{1}H NMR (400 MHz, MeOH-d_4): 8.11 (s, 1H), 7.13 (d, J = 3.6 Hz, 1H), 6.69 (d, J = 3.6 Hz, 1H), 3.56-3.60 (m, 1H), 3.36 (s, 3H), 3.02 (q, J = 7.2 Hz, 2H), 2.70-2.77 (m, 2H), 2.25-2.33 (m, 2H), 1.18 (t, J = 7.2 Hz, 3H). (The H_2O peak at δ 4.90 obscures a methine proton signal.) LC/MS m/z (M + H$^+$) calcd for $C_{13}H_{21}N_6O_2S$: 325. Found: 325.

***N*-Prop-1-yl-*N*'-{*cis*-3-[methyl(7*H*-pyrrolo[2,3-*d*]pyrimidin-4-yl)amino]cyclobutyl}sulfamide (12).** This sulfamide analog was prepared using a procedure similar to that used to prepare compound **14**, starting with intermediate **50**. ^{1}H NMR (400 MHz, MeOH-d_4): 8.12 (s, 1H), 7.12 (d, J = 3.6 Hz, 1H), 6.69 (d, J = 3.6 Hz, 1H), 3.53-3.62 (m, 1H), 3.36 (s, 3H), 2.93 (t, J = 7.2 Hz, 2H), 2.70-2.77 (m, 2H), 2.25-2.33 (m, 2H), 1.54-1.63 (m, 2H), 1.18 (t, J = 7.2 Hz, 3H). (The H_2O peak at 4.90 obscures a methine proton signal.) LC/MS m/z (M + H$^+$) calcd for $C_{14}H_{23}N_6O_2S$: 339. Found: 339.

***N*-Cyclopropyl-*N*'-{*cis*-3-[methyl(7*H*-pyrrolo[2,3-*d*]pyrimidin-4-yl)amino]cyclobutyl}sulfamide (13).** This sulfamide analog was prepared using a procedure

similar to that used to prepare compound **14**, starting with intermediate **50**. ^{1}H NMR (400 MHz, DMSO-d_6): 11.66 (br s, 1H), 8.09 (s, 1H), 7.39 (d, J = 8.8 Hz, 1H), 7.24 (br s, 1H), 7.14-7.15 (m, 1H), 6.61-6.62 (m, 1H), 4.86-4.95 (m, 1H), 3.40-3.46 (m, 1H, overlapped), 3.25 (s, 3H), 2.50-2.57 (m, 2H, overlapped), 2.22-2.29 (m, 3H), 0.50-0.54 (m, 4H). LC/MS m/z (M + H^+) calcd for $C_{14}H_{21}N_6O_2S$: 337. Found: 337.

***N*-(Cyclopropylmethyl)-*N*'-{*cis*-3-[methyl(7*H*-pyrrolo[2,3-*d*]pyrimidin-4-yl)amino]cyclobutyl}sulfamide (14).** *Step 1:* A solution of **50** (150 mg, 0.29 mmol), cyclopropanemethylamine (51 mg, 0.72 mmol) and TEA (116 mg, 1.15 mmol) in MeCN (3 mL) was stirred for 15 min at 100°C in a sealed tube under microwave heating. The reaction mixture was concentrated to afford the crude *N*-(cyclopropylmethyl)-*N′*-[*cis*-3-(methyl{7-[(4-methylphenyl)-sulfonyl]-7*H*-pyrrolo[2,3-*d*]pyrimidin-4-yl}amino)cyclobutyl]sulfamide (146 mg, 100% crude yield) as a yellow oil. LC/MS m/z (M + H^+) calcd for $C_{22}H_{29}N_6O_4S_2$: 505. Found: 505.

Step 2: A solution of *N*-(cyclopropylmethyl)-*N′*-[*cis*-3-(methyl{7-[(4-methylphenyl)sulfonyl]-7*H*-pyrrolo[2,3-*d*]pyrimidin-4-yl}amino)cyclobutyl]sulfamide (146 mg, 0.29 mmol), LiOH.H_2O (48 mg, 1.14 mmol) in EtOH (5 mL) and H_2O (2.5 mL) was stirred at 100°C for 1 h. The reaction mixture was concentrated under vacuum and the crude product was purified by preparative HPLC to afford the title compound (14 mg, 14%) as a white solid. ^{1}H NMR (400 MHz, MeOH-d_4): 8.12 (s, 1H), 7.12 (d, J = 3.6 Hz, 1H), 6.69 (d, J = 3.6 Hz, 1H), 3.59-3.63 (m, 1H), 3.37 (s, 3H), 2.84 (d, J = 7.2 Hz, 2H), 2.71-2.78 (m, 2H), 2.26-2.33 (m, 2H), 1.03-1.05 (m, 1H), 0.52-0.57 (m, 2H); 0.25-0.30 (m, 2H). (The H_2O peak at 4.90 obscures a methine proton signal.) LC/MS m/z (M + H^+) calcd for $C_{15}H_{23}N_6O_2S$: 351. Found: 351.

***N*-(3-Cyanoprop-1-yl)-*N*'-{*cis*-3-[methyl(7*H*-pyrrolo[2,3-*d*]pyrimidin-4-yl)amino]cyclobutyl}sulfamide (15).** This sulfamide analog was prepared using a procedure similar to that used to prepare compound **14**, starting with intermediate **50**. ^{1}H NMR (400 MHz, MeOH-d_4): 8.11 (s, 1H), 7.12 (d, J = 3.6 Hz, 1H), 6.68 (d, J = 3.6 Hz, 1H), 4.88-4.92 (m, 1H, overlapped), 3.57-3.63 (m, 1H), 3.36 (s, 3H), 3.10 (t, J = 6.6 Hz, 2H), 2.72-2.78 (m, 2H), 2.59 (t, J = 7.2 Hz, 2H), 2.27-2.34 (m, 2H), 1.87-1.94 (m, 2H). LC/MS m/z (M + H$^+$) calcd for $C_{15}H_{22}N_7O_2S$: 364. Found: 364.

***N*-Methyl-*N*-{*cis*-3-[(ethylsulfonyl)methyl]cyclobutyl}-7*H*-pyrrolo[2,3-*d*]pyrimidin-4-amine (16)**. *Step 1:* A solution of **56** (489 mg, 1.11 mmol) in MeOH (5.5 mL) was cooled in an ice bath and sparged with N_2 for 10 min. Subsequently, K_2CO_3 (608 mg, 4.39 mmol) and $NaBH_4$ (166 mg, 4.4 mmol) were added and the resulting mixture was stirred at 0°C for 3 h. Ethyl iodide (0.22 mL, 2.74 mmol) was added. The reaction mixture was stirred overnight, allowing it to warm to rt, and then quenched by addition of 1M aq. HCl solution. The mixture was extracted three times with EtOAc and the combined organic extracts were dried over $MgSO_4$ and concentrated under vacuum. The crude product mixture was chromatographed eluting with a gradient of 5-100% EtOAc/heptane to provide *N*-{*cis*-3-[(ethylthio)methyl]cyclobutyl}-*N*-methyl-7-tosyl-7*H*-pyrrolo[2,3-*d*]pyrimidin-4-amine as an oil (200 mg, 42%). ^{1}H NMR (400 MHz, MeOH-d_4): 8.22 (s, 1H), 8.00 (d, J = 8.6 Hz, 2H), 7.57 (d, J = 4.3 Hz, 1H), 7.39 (d, J = 8.2 Hz, 2H), 6.89 (d, J = 3.9 Hz, 1H), 4.89-4.99 (m, 1H), 3.28 (s, 3H), 2.69 (d, J = 7.0 Hz, 2H), 2.57 (q, J = 7.4 Hz, 2H), 2.43-2.52 (m, 2H), 2.41 (s, 3H), 2.24-2.32 (m, 1H), 1.96-2.05 (m, 2H), 1.27 (t, J = 7.4 Hz, 3H).

Step 2: *N*-{*cis*-3-[(Ethylthio)methyl]cyclobutyl}-*N*-methyl-7-tosyl-7*H*-pyrrolo[2,3-*d*]pyrimidin-4-amine (200 mg, 0.46 mmol) was dissolved in EtOH (4.6 mL) and H_2O (2.3 mL). The mixture

was treated with $LiOH \cdot H_2O$ (98 mg, 2.33 mmol) and heated at 70°C overnight. The solvents were evaporated under vacuum and the residue was taken up in 1M aq. NaOH solution. The mixture was extracted three times with EtOAc and the combined organic layers were dried over $MgSO_4$ and concentrated. The desired product, *N*-(*cis*-3-{[ethylthio)methyl]cyclobutyl}-*N*-methyl-7*H*-pyrrolo[2,3-*d*]pyrimidin-4-amine (110 mg, 86%), was isolated by flash chromatography eluting with a gradient of 5-100% EtOAc/heptane. ^{1}H NMR (400 MHz, DMSO-d_6): 11.61 (br s, 1H), 8.11 (s, 1H), 7.15 (dd, *J* = 2.3, 3.5 Hz, 1H), 6.61 (dd, *J* = 1.6, 3.5 Hz, 1H), 5.04-5.13 (m, 1H), 3.25 (s, 3H), 2.68 (d, *J* = 7.0 Hz, 2H), 2.53 (q, *J* = 7.4 Hz, 2H, overlapped by solvent peak), 2.32-2.39 (m, 2H), 2.16-2.27 (m, 1H), 1.93-2.01 (m, 2H), 1.21 (t, *J* = 7.4 Hz, 3H).

Step 3: *N*-(*cis*-3-{[Ethylthio)methyl]cyclobutyl}-*N*-methyl-7*H*-pyrrolo[2,3-*d*]pyrimidin-4-amine (55 mg, 0.20 mmol) was dissolved in a mixture of THF (2 mL) and EtOH (2 mL). The mixture was cooled in an ice bath and then a solution of Oxone® (342 mg, 1.11 mmol) in water (2 mL) was added dropwise over 30 min. The cooling bath was removed and the reaction mixture was stirred for another 2.5 h, warming to rt during this period. The reaction was quenched with 10% aq. $NaHSO_3$ solution (20 mL). Saturated aq. $NaHCO_3$ (30 mL) was added to adjust the pH to ~7 and the resulting mixture was quenched three times with EtOAc. The combined organic extracts were dried over $MgSO_4$ and concentrated under vacuum to provide the title compound (48 mg, 80%) as a white solid. ^{1}H NMR (400 MHz, $CDCl_3$): 11.73, (br s, 1H), 8.23 (s, 1H), 7.17 (dd, *J* = 1.8, 3.5 Hz, 1H), 6.64 (dd, *J* = 1.6, 3.5 Hz, 1H), 5.15-5.23 (m, 1H), 3.46 (s, 3H), 3.16 (d, *J* = 7.0 Hz, 2H), 3.01 (q, *J* = 7.4 Hz, 2H), 2.66-2.81 (overlapping m, 3H), 2.18-2.25 (m, 2H), 1.44 (t, *J* = 7.4 Hz, 3H). LC/MS m/z ($M + H^+$) calcd for $C_{14}H_{21}N_4O_2S$: 309. Found: 309. Purity (LC/MS) = 90% (UV), 100% (ELSD).

_N_-Methyl-_N_-{_cis_-3-[(cyclopropylsulfonyl)methyl]cyclobutyl}-7_H_-pyrrolo[2,3-_d_]pyrimidin-4-amine (17). This sulfone analog was made in a manner similar to that used to prepare compound **19** starting with intermediate **55b**. ^{1}H NMR (400 MHz, $CDCl_3$): 11.59, (br s, 1H), 8.26 (s, 1H), 7.20-7.21 (m, 1H), 6.66-6.67 (m, 1H), 5.21 (br s, 1H), 3.46 (s, 3H), 3.26 (d, J = 6.8 Hz, 2H), 2.70-2.80 (m, 3H), 2.35-2.41 (m, 1H), 2.20 (br s, 2H), 1.25-1.30 (m, 2H), 1.05-1.11 (m, 2H). LC/MS m/z (M + H^+) calcd for $C_{15}H_{21}N_4O_2S$: 321. Found: 321.

_N_-Methyl-_N_-{_cis_-3-[(propylsulfonyl)methyl]cyclobutyl}-7_H_-pyrrolo[2,3-_d_]pyrimidin-4-amine (18). This sulfone analog was made in a manner similar to that used to prepare compound **16** starting with intermediate **56**. ^{1}H NMR (400 MHz, MeOH-d_4): 8.11 (s, 1H), 7.11 (d, J = 3.6 Hz, 1H), 6.68 (d, J = 3.6 Hz, 1H), 5.07-5.16 (m, 1H), 3.36 (s, 3H), 3.03-3.07 (m, 2H), 2.57-2.65 (m, 3H), 2.17-2.26 (m, 2H), 1.80-1.89 (m, 2H), 1.10 (t, J = 7.2 Hz, 3H). (The solvent peak at δ 3.31 obscures a methylene proton signal.) LC/MS m/z (M + H^+) calcd for $C_{15}H_{23}N_4O_2S$: 323. Found: 323.

_N_-{_cis_-3-[(Butylsulfonyl)methyl]cyclobutyl}-_N_-methyl-7_H_-pyrrolo[2,3-_d_]pyrimidin-4-amine (19). *Step 1:* A solution of **55a** (23 g, 42.6 mmol) was stirred in NMP (100 mL). DBU (12.8 g, 85.2 mmol) and 1-butanethiol (7.8 g, 85.2 mmol) was added to the reaction mixture. The reaction was stirred at rt for 16 h. H_2O (200 mL) and EtOAc (500 mL) were added. The aqueous layer was extracted with EtOAc (2 x 500 mL) and the combined organic layers were dried and concentrated. The residue was chromatographed eluting with a gradient of DCM and MeOH (100:0 to 90:10) to afford _N_-{_cis_-3-[(butylthio)methyl]cyclobutyl}-_N_-methyl-7_H_-pyrrolo[2,3-_d_]pyrimidin-4-amine (11.8 g, 91%). LC/MS m/z (M + H^+) calcd for $C_{16}H_{25}N_4S$: 305. Found: 305.

Step 2: N-{*cis*-3-[(Butylthio)methyl]cyclobutyl}-*N*-methyl-7*H*-pyrrolo[2,3-*d*]pyrimidin-4-amine (12 g, 39.5 mmol) was dissolved in a mixture of THF (200 mL), EtOH (200 mL) and H_2O (200 mL). Oxone® (48.6 g, 158 mmol) was added and the reaction was stirred at rt for 1 h. The mixture was then filtered, washing the solids with a mixture of THF (40 mL), EtOH (40 mL) and H_2O (20 mL). The filtrate was treated with 10% aq. $NaHSO_3$ solution (200 mL) and stirred at rt for 20 min. Saturated aq. $NaHCO_3$ was added to adjust the pH to ~7. The mixture was extracted with DCM (3 x 800 mL) and the combined organic layers were dried and concentrated under vacuum. The crude residue was chromatographed eluting with a gradient of DCM and MeOH (100:0 to 95:5) to obtain the title compound (11.4 g, 86%). ^{1}H NMR (400 MHz, DMSO-d_6): 11.63, (br s, 1H), 8.12 (s, 1H), 7.15-7.17 (m, 1H), 6.63-6.65 (m, 1H), 5.10-5.19 (m, 1H), 3.35 (d, J = 7.0 Hz, 2H), 3.27 (s, 3H), 3.03-3.07 (m, 2H), 2.41-2.50 (m, 3H), 2.11-2.21 (m, 2H), 1.64-1.72 (m, 2H), 1.48-1.57 (m, 2H), 0.92 (t, J = 7.4 Hz, 3H). LC/MS m/z (M + H^+) calcd for $C_{16}H_{25}N_4O_2S$: 337. Found: 337.

***N*-{*cis*-3-[(Phenylsulfonyl)methyl]cyclobutyl}-*N*-methyl-7*H*-pyrrolo[2,3-*d*]pyrimidin-4-amine (20).** This sulfone analog was prepared in a manner similar to that used to prepare compound **19**, starting with intermediate **55b.** ^{1}H NMR (400 MHz, $CDCl_3$): 11.01, (br s, 1H), 8.30 (s, 1H), 7.94 (d, J = 6.8 Hz, 2H), 7.65-7.68 (m, 1H), 7.57-7.61 (m, 2H), 7.07 (d, J = 3.6 Hz, 1H), 6.54 (d, J = 3.6 Hz, 1H), 5.09-5.14 (m, 1H), 3.30 (d, J = 6.8 Hz, 2H, overlapped), 3.29 (s, 3H), 2.45-2.54 (m, 2H), 2.36-2.43 (m, 1H), 1.99-2.02 (m, 2H). LC/MS m/z (M + H^+) calcd for $C_{18}H_{21}N_4O_2S$: 357. Found: 357.

***N*-Ethyl-1-{*cis*-3-[methyl(7*H*-pyrrolo[2,3-*d*]pyrimidin-4-yl)amino]cyclobutyl}methanesulfonamide (21).** This reverse sulfonamide analog was prepared in parallel chemistry format in a manner similar to that used to prepare compound **43**. LC/MS

m/z (M + H^+) calcd for $C_{14}H_{22}N_5O_2S$: 324. Found: 324. Purity (HPLC) = 87% (UV), 98.1% (ELSD).

1-{*cis*-3-[Methyl(7*H*-pyrrolo[2,3-*d*]pyrimidin-4-yl)amino]cyclobutyl}-*N*-propylmethanesulfonamide (22). This reverse sulfonamide analog was prepared in parallel chemistry format in a manner similar to that used to prepare compound **43**. LC/MS m/z (M + H^+) calcd for $C_{15}H_{24}N_5O_2S$: 338. Found: 338.

***N*-Butyl-1-{*cis*-3-[methyl(7*H*-pyrrolo[2,3-*d*]pyrimidin-4-yl)amino]cyclobutyl}methanesulfonamide (23).** This reverse sulfonamide analog was prepared in parallel chemistry format in a manner similar to that used to prepare compound **43**. LC/MS m/z (M + H^+) calcd for $C_{16}H_{26}N_5O_2S$: 352. Found: 352. Purity (HPLC) = 94% (UV), 100% (ELSD).

***N*-(Cyclopropylmethyl)-1-{*cis*-3-[methyl(7*H*-pyrrolo[2,3-*d*]pyrimidin-4-yl)amino]cyclobutyl}methanesulfonamide (24).** This reverse sulfonamide analog was prepared in parallel chemistry format in a manner similar to that used to prepare compound **43**. LC/MS m/z (M + H^+) calcd for $C_{16}H_{24}N_5O_2S$: 350. Found: 350. Purity (HPLC) = 90% (UV), 98.9% (ELSD).

***N*-{*cis*-3-[Methyl(7*H*-pyrrolo[2,3-*d*]pyrimidin-4-yl)amino]cyclobutyl}propane-1-sulfonamide (25).**[37] Compound **48a**·2HBr (125 g, 0.234 mol) was added in portions to a mixture of 2-MeTHF (1.25 L) and TEA (442 mL, 3.17 mol). The resulting mixture was stirred at rt for 1 h and then 1-propanesulfonyl chloride (45 mL, 0.40 mol) was added over 10 min. The reaction mixture was stirred for 1 h at rt and then washed with 10% aq. citric acid solution (2 x 1.25 L).

Aqueous 3M NaOH solution (1.25 L, 3.75 mol) was combined with the organic layer in a reaction vessel and the resulting mixture was heated to reflux with stirring for 1 h.

The reaction mixture was allowed to cool to rt and which point the layers were separated. The organic layer was extracted with 3M aq. NaOH (2 x 60 mL). All aqueous phases were combined and cooled to 15°C in an ice bath. Acidification to ~pH 6 was carried out by slow addition of aq. 6M HCl solution (~1.3 L). During the addition, precipitation of the desired product took place. The resulting slurry was cooled to 5°C and stirred for 1 h at this temperature. The title compound, a tan granular solid (66.2 g, 87%) was collected by filtration, washed with H_2O (500 mL), and dried overnight in a vacuum oven at 40°C. The material was recrystallized from a mixture of EtOH (442 mL) and H_2O (221 mL), heating to reflux until all solids dissolved and allowing the solution to cool slowly to rt. The title compound (56.2 g, 74%) was collected by filtration, washed with 2:1 EtOH/H_2O (100 mL) and again dried overnight in a vacuum oven at 40°C. ^{1}H NMR (400 MHz, DMSO-d_6): 11.64 (br s, 1H), 8.12 (s, 1 H), 7.50 (d, J = 9.4 Hz, 1H), 7.10-7.22 (m, 1H), 6.65 (dd, J = 1.8, 3.3 Hz, 1H), 4.87-4.96 (m, 1H), 3.53-3.64 (m, 1H), 3.27 (s, 3H), 2.93-2.97 (m, 2H), 2.57-2.64 (m, 2H), 2.20-2.28 (m, 2H), 1.65-1.74 (m, 2H), 0.99 (t, J = 7.4 Hz, 3H). LC/MS m/z (M + H^+) calcd for $C_{14}H_{22}N_5O_2S$: 324. Found: 324. Anal. calcd for $C_{14}H_{21}N_5O_2S$: C, 51.99; H, 6.54; N, 21.65; O, 9.89; S, 9.91. Found: C, 52.06; H, 6.60; N, 21.48; O, 10.08; S, 9.97.

***N*-{*trans*-3-[Methyl(7*H*-pyrrolo[2,3-*d*]pyrimidin-4-yl)amino]cyclobutyl}propane-1-sulfonamide (26).** This compound was made starting with *trans*-**45**, which was combined with compound **46a** and advanced as described for the preparation of **25**. ^{1}H NMR (400 MHz, DMSO-d_6): 11.64 (br s, 1H), 8.11 (s, 1H), 7.66 (d, J = 7.2 Hz, 1H), 7.15-7.17 (m, 1H), 6.60-6.62 (m, 1H), 5.42-5.46 (m, 1H), 3.85-3.87 (m, 1H), 3.26 (s, 3H), 2.93-2.96 (m, 2H), 2.60-2.67 (m,

2H), 2.27-2.33 (m, 2H), 1.63-1.71 (m, 2H), 0.98 (t, J = 7.6 Hz, 3H). LC/MS m/z (M + H^+) calcd for $C_{14}H_{22}N_5O_2S$: 324. Found: 324.

***N*-(*cis*-3-(Methyl(7*H*-pyrrolo[2,3-*d*]pyrimidin-4-yl)amino)cyclobutyl)butane-1-sulfonamide (27).** This sulfonamide analog was prepared using a procedure similar to that used to prepare compound **25** starting from **48a**·HBr. ^{1}H NMR (400 MHz, DMSO-d_6): 11.63 (br s, 1H), 8.10 (s, 1H), 7.49 (d, *J* = 9.1 Hz, 1H), 7.15 (dd, *J* = 2.5, 3.5 Hz, 1H), 6.64 (dd, *J* = 1.9, 3.5 Hz, 1H), 4.86-4.95 (m, 1H), 3.52-3.63 (m, 1H), 3.26 (s, 3H), 2.93-2.97 (m, 2H), 2.55-2.62 (m, 2H), 2.19-2.27 (m, 2H), 1.60-1.68 (m, 2H), 1.35-1.44 (m, 2H), 0.89 (t, J = 7.3 Hz, 3H). LC/MS m/z (M + H^+) calcd for $C_{15}H_{24}N_5O_2S$: 338. Found: 338. Purity (HPLC) = 100% (UV), 92.0% (ELSD).

***N*-(*cis*-3-(Methyl(7*H*-pyrrolo[2,3-*d*]pyrimidin-4-yl)amino)cyclobutyl)cyclopropanesulfonamide (28).** This sulfonamide analog was prepared using a procedure similar to that used to prepare compound **25** starting from **48a**·HBr. ^{1}H NMR (400 MHz, DMSO-d_6): 11.63 (br s, 1H), 8.10 (s, 1H), 7.48 (d, *J* = 9.6 Hz, 1H), 7.15 (dd, *J* = 2.5, 3.5 Hz, 1H), 6.64 (dd, *J* = 1.8, 3.5 Hz, 1H), 4.90-4.99 (m, 1H), 3.54-3.65 (m, 1H), 3.26 (s, 3H), 2.56-2.63 (m, 2H), 2.44-2.48 (m, 1H, overlapped), 2.22-2.30 (m, 2H), 0.91-0.97 (m, 4H). LC/MS m/z (M + H^+) calcd for $C_{14}H_{20}N_5O_2S$: 322. Found: 322.

1-Cyclopropyl-*N*-(*cis*-3-(methyl(7*H*-pyrrolo[2,3-*d*]pyrimidin-4-yl)amino)cyclobutyl)methanesulfonamide (29). This sulfonamide analog was prepared using a procedure similar to that used to prepare compound **25** starting from **48a**·HBr. ^{1}H NMR (400 MHz, DMSO-d_6): 11.63 (br s, 1H), 8.10 (s, 1H), 7.52 (d, *J* = 9.4 Hz, 1H), 7.14-7.15 (m, 1H), 6.63-6.64 (m, 1H), 4.85-4.94 (m, 1H), 3.55-3.65 (m, 1H), 3.26 (s, 3H), 2.91 (d, *J* = 7.0 Hz, 2H), 2.57-2.63 (m, 2H), 2.21-2.28 (m, 2H), 0.97-1.09 (m, 1H), 0.56-0.61 (m, 2H), 0.32-0.36 (m, 2H).

LC/MS m/z (M + H^+) calcd for $C_{15}H_{22}N_5O_2S$: 336. Found: 336. Anal. calcd for $C_{15}H_{21}N_5O_2S$: C, 53.71; H, 6.31; N, 20.88; S, 9.56. Found: C, 53.42; H, 6.46; N, 20.10; S, 9.33.

1-Cyclobutyl-*N*-(*cis*-3-(methyl(7*H*-pyrrolo[2,3-*d*]pyrimidin-4-yl)amino)cyclobutyl)methanesulfonamide (30). This sulfonamide analog was prepared using a procedure similar to that used to prepare compound **25** starting from **48a**·HBr. ^{1}H NMR (400 MHz, DMSO-d_6): 12.37 (br s, 1H), 8.28 (s, 1H), 7.47 (d, J = 9.0 Hz, 1H), 7.37 (br s, 1H), 6.88 (br s, 1H), 4.66-4.89 (m, 1H), 3.49-3.71 (m, 1H), 3.33 (s, 3H), 3.08 (d, J = 7.0 Hz, 2H), 2.58-2.76 (m, 3H), 2.20-2.37 (m, 2H), 2.01-2.15 (m, 2H), 1.71-1.95 (m, 4H). LC/MS m/z (M + H^+) calcd for $C_{16}H_{24}N_5O_2S$: 350. Found: 350. Purity (HPLC) = 100% (UV), 88% (ELSD).

3,3,3-Trifluoro-*N*-(*cis*-3-(methyl(7*H*-pyrrolo[2,3-*d*]pyrimidin-4-yl)amino)cyclobutyl)propane-1-sulfonamide (31). To a solution of **48b** (80 mg, 0.37 mmol) in THF (6 mL) and H_2O (2 mL) was added K_2CO_3 (150 mg, 1.1 mmol) and 3,3,3-trifluoropropane-1-sulfonyl chloride (95 mg, 0.48 mmol) at 0°C. The reaction was stirred at rt overnight and then concentrated to dryness. The residue was purified by prep-HPLC to afford the title compound (37 mg, 26%) as white solid. ^{1}H NMR (400 MHz, DMSO-d_6): 8.13 (s, 1H), 7.12 (d, J = 3.6 Hz, 1H), 6.70 (d, J = 3.6 Hz, 1H), 4.96 (m, 1H), 3.76 (m, 1H), 3.33 (s, 3H), 3.26 (m, 2H), 2.80 (m, 2H), 2.65 (m, 2H), 2.25 (m, 2H). LC/MS m/z (M + H^+) calcd for $C_{14}H_{19}F_3N_5O_2S$: 378. Found: 378.

4,4,4-Trifluoro-*N*-(*cis*-3-(methyl(7*H*-pyrrolo[2,3-*d*]pyrimidin-4-yl)amino)cyclobutyl)butane-1-sulfonamide (32). This sulfonamide analog was prepared using a procedure similar to that used to prepare compound **31** starting from **48b**. White solid, 21% yield. ^{1}H NMR (400 MHz, DMSO-d_6): (all broadened unresolved peaks) 11.64 (1H), 8.10 (1H),

7.66 (1H), 7.15 (1H), 6.64 (1H), 4.90 (1H), 3.59 (1H), 3.25 (3H), 3.10 (2H), 2.35 (2H), 1.89 (2H) (other signals overlapped by DMSO signal at 2.50 or H_2O peak at 3.35). LC/MS m/z ($M + H^+$) calcd for $C_{15}H_{21}F_3N_5O_2S$: 392. Found: 392.

2-Methoxy-*N*-(*cis*-3-(methyl(7*H*-pyrrolo[2,3-*d*]pyrimidin-4-yl)amino)cyclobutyl)ethanesulfonamide (33). This sulfonamide analog was prepared using a procedure similar to that used to prepare compound **25** starting from **48a**·HBr. ^{1}H NMR (400 MHz, DMSO-d_6): 11.63 (br s, 1H), 8.10 (s, 1H), 7.55 (d, J = 9.1 Hz, 1H), 7.14-7.16 (m, 1H), 6.63-6.64 (m, 1H), 4.86-4.95 (m, 1H), 3.67 (t, J = 6.4 Hz, 2H), 3.54-3.63 (m, 1H), 3.27 (s, 3H), 3.25 (s, 3H), 3.25 (t, J = 6.4 Hz, 2H, overlapped), 2.55-2.63 (m, 2H), 2.21-2.28 (m, 2H). LC/MS m/z ($M + H^+$) calcd for $C_{14}H_{22}N_5O_3S$: 340. Found: 340.

3-Methoxy-*N*-(*cis*-3-(methyl(7*H*-pyrrolo[2,3-*d*]pyrimidin-4-yl)amino)cyclobutyl)propane-1-sulfonamide (34). This sulfonamide analog was prepared using a procedure similar to that used to prepare compound **31** starting from **48b**. White solid, 39% yield. ^{1}H NMR (400 MHz, DMSO-d_6): 11.63 (br s, 1H), 8.10 (s, 1H), 7.55 (d, J = 9.2 Hz, 1H), 7.14 (br s, 1H), 6.64 (br s, 1H), 4.86-4.95 (m, 1H), 3.54-3.60 (m, 1H), 3.39-3.42 (m, 2H, overlapped), 3.25 (s, 3H), 3.22 (s, 3H), 2.97-3.00 (m, 2H), 2.57-2.59 (m, 2H), 2.19-2.26 (m, 2H), 1.85-1.91 (m, 2H). LC/MS m/z ($M + H^+$) calcd for $C_{15}H_{24}N_5O_3S$: 354. Found: 354.

3-Cyano-*N*-(*cis*-3-(methyl(7*H*-pyrrolo[2,3-*d*]pyrimidin-4-yl)amino)cyclobutyl)propane-1-sulfonamide (35). This sulfonamide analog was prepared using a procedure similar to that used to prepare compound **25** starting from **48a**·HBr. In this case the *N*-tosyl group was removed by heating with Cs_2CO_3 (3 eq.) in EtOH at ~85°C overnight (sealed vessel). ^{1}H NMR (400 MHz, DMSO-d_6): 11.64 (br s, 1H), 8.12 (s, 1H), 7.68 (d, J = 9.4 Hz, 1H), 7.15-7.17 (m, 1H), 6.49-6.74

(m, 1H), 4.88-4.97 (m, 1H), 3.55-3.65 (m, 1H), 3.33 (s, 3H), 3.06-3.10 (m, 2H), 2.69 (t, J = 7.2 Hz, 2H), 2.59-2.65 (m, 2H), 2.21-2.29 (m, 2H), 1.92-2.00 (m, 2H). LC/MS m/z ($M + H^+$) calcd for $C_{15}H_{21}N_6O_2S$: 349. Found: 349.

***N*-{*cis*-3-[Methyl(7*H*-pyrrolo[2,3-*d*]pyrimidin-4-yl)amino]cyclobutyl}-1-oxetan-3-ylmethanesulfonamide (36).** To a solution of **48b**·HCl (1.38 g, 5.4 mmol) in THF (20 mL) was added a 1M solution of LiHMDS in THF (13.8 mL, 13.8 mmol). After 10 min, TMSCl (1.08 g, 10 mmol) was added. The resulting mixture was stirred at rt for 1h at which point a solution of oxetan-3-ylmethanesulfonyl chloride (0.85 g, 5 mmol) in THF (5 mL) was added dropwise. The reaction mixture was stirred at rt for 8 h and then was quenched by addition of aq. NH_4Cl solution. The mixture was extracted with twice with 3:1 DCM/*i*-PrOH (2 x 150 ml), and the combined organic layers were dried over Na_2SO_4 and concentrated. The crude product was purified by flash chromatography eluting with 7% MeOH/DCM to afford the title compound as white solid (700 mg, 39%). The compound was recrystallized from EtOH (612 mg, 34%). ^{1}H NMR (400 MHz, DMSO-d_6): 11.64 (br s, 1H), 8.12 (s, 1H), 7.61 (d, J = 9.0 Hz, 1H), 7.15-7.17 (m, 1H), 6.64-6.66 (m, 1H), 4.87-4.95 (m,1H), 4.65-4.68 (m, 2H), 4.44-4.47 (m, 2H), 3.54-3.64 (m, 1H), 3.56-3.58 (m, 1H), 3.35-3.49 (m, 2H), 3.27 (s, 3H), 2.56-2.68 (m, 2H), 2.20-2.28 (m, 2H). LC/MS m/z ($M + H^+$) calcd for $C_{15}H_{22}N_5O_3S$: 352. Found: 352.

[Oxetan-3-ylmethanesulfonyl chloride was prepared as follows. To a solution of oxetan-3-ylmethyl 4-methylbenzenesulfonate (4.8 g, 20 mmol) in EtOH (100 mL) was added KSCN (2.91 g, 30 mmol) at rt.[38] The mixture was heated to reflux for 12 h giving a clear solution. The mixture was concentrated to afford a white solid containing oxetan-3-ylmethyl thiocyanate. This was taken up H_2O (25 mL) and cooled to 0°C. Chlorine gas was then bubbled through the mixture for about 30 min giving a yellow solution. The mixture as extracted twice with MTBE (2

x 100 mL). The combined organic layers were washed with H_2O (4 x 10 mL) and concentrated to afford crude oxetan-3-ylmethanesulfonyl chloride as yellow oil (1.7g, 50%), used without further purification. ^{1}H NMR (400 MHz, $CDCl_3$): 4.60 (dd, *J* = 7.2, 9.6 Hz, 2H), 4.34 (dd, *J* = 6.4, 9.6 Hz, 2H), 3.74 (d, J = 6.4 Hz, 2H), 3.31-3.40 (m, 1H).]

***N*-Ethyl-*N*-methyl-*N*'-{*cis*-3-[methyl(7*H*-pyrrolo[2,3-*d*]pyrimidin-4-yl)amino]cyclobutyl}sulfamide (37).** This sulfamide analog was prepared using a procedure similar to that used to prepare compound **14**, starting with intermediate **50**. ^{1}H NMR (400 MHz, MeOH-d_4): 8.11 (s, 1H), 7.11 (d, *J* = 3.6 Hz, 1H), 6.68 (d, *J* = 3.6 Hz, 1H), 3.54-3.61 (m, 1H), 3.34 (s, 3H), 3.20 (q, *J* = 7.2 Hz, 2H), 2.78 (s, 3H), 2.68-2.75 (m, 2H), 2.23-2.30 (m, 2H), 1.19 (t, *J* = 7.2 Hz, 3H). (The H_2O peak at 4.90 obscures a methine proton signal.) LC/MS m/z (M + H^+) calcd for $C_{14}H_{23}N_6O_2S$: 339. Found: 339.

***N*-Cyclopropyl-*N*-methyl-*N*'-{*cis*-3-[methyl(7*H*-pyrrolo[2,3-*d*]pyrimidin-4-yl)amino]cyclobutyl}sulfamide (38).** This sulfamide analog was prepared using a procedure similar to that used to prepare compound **14**, starting with intermediate **50**. ^{1}H NMR (400 MHz, MeOH-d_4): 8.10 (s, 1H), 7.11 (d, *J* = 3.6 Hz, 1H), 6.68 (d, *J* = 3.6 Hz, 1H), 4.80-4.89 (m, 1H), 3.60-3.68 (m, 1H), 3.35 (s, 3H), 2.81 (s, 3H), 2.68-2.74 (m, 2H), 2.25-2.32 (m, 3H), 0.73-0.74 (m, 4H). LC/MS m/z (M + H^+) calcd for $C_{15}H_{23}N_6O_2S$: 351. Found: 351.

***N*-(*cis*-3-(Methyl(7*H*-pyrrolo[2,3-*d*]pyrimidin-4-yl)amino)cyclobutyl)piperidine-1-sulfonamide (39).** This sulfamide analog was prepared using a procedure similar to that used to prepare compound **14**, starting with intermediate **50**. ^{1}H NMR (400 MHz, DMSO-d_6): 11.62 (br s, 1H), 8.10 (s, 1H), 7.57 (d, *J* = 9.1 Hz, 1H), 7.13-7.15 (m, 1H), 6.63-6.64 (m, 1H), 4.85-4.94 (m, 1H), 3.57 (s, 3H), 3.45-3.54 (m, 1H), 2.99-3.02 (m, 4H), 2.50-2.57 (m, 2H, overlapped),

2.17-2.25 (m, 2H), 1.51-1.57 (br m, 4H), 1.43-1.50 (m, 2H). LC/MS m/z (M + H^+) calcd for $C_{16}H_{25}N_6O_2S$: 365. Found: 365.

***N*-(2-Cyanoethyl)-*N*-methyl-*N'*-{*cis*-3-[methyl(7*H*-pyrrolo[2,3-*d*]pyrimidin-4-yl)amino]cyclobutyl}sulfamide (40).** This sulfamide analog was prepared using a procedure similar to that used to prepare compound **14**, starting with intermediate **50**. ^{1}H NMR (400 MHz, DMSO-d_6): 11.63 (br s, 1H), 8.10 (s, 1H), 7.73 (d, J = 9.0 Hz, 1H), 7.14-7.16 (m, 1H), 6.63-6.64 (m, 1H), 4.87-4.96 (m, 1H), 3.49-3.59 (m, 1H), 3.33 (t, J = 6.6 Hz, 2H, overlapped by H_2O peak), 3.26 (s, 3H), 2.80 (t, J = 6.6 Hz, 2H), 2.75 (s, 3H), 2.53-2.59 (m, 2H, overlapped by solvent peak), 2.18-2.28 (m, 2H). LC/MS m/z (M + H^+) calcd for $C_{15}H_{22}N_7O_2S$; 364. Found: 364.

***N*-Butyl-*N*-methyl-1-{*cis*-3-[methyl(7*H*-pyrrolo[2,3-*d*]pyrimidin-4-yl)amino]cyclobutyl}methanesulfonamide (41).** This reverse sulfonamide analog was prepared in parallel chemistry format in a manner similar to that used to prepare compound **43**. LC/MS m/z (M + H^+) calcd for $C_{17}H_{28}N_5O_2S$: 366. Found: 366.

***N*-(Cyclopropylmethyl)-*N*-methyl-1-{*cis*-3-[methyl(7*H*-pyrrolo[2,3-*d*]pyrimidin-4-yl)amino]cyclobutyl}methanesulfonamide (42).** This reverse sulfonamide analog was prepared in parallel chemistry format in a manner similar to that used to prepare compound **43**. LC/MS m/z (M + H^+) calcd for $C_{17}H_{26}N_5O_2S$: 364. Found: 364.

***N*-methyl-*N*-{*cis*-3-[(pyrrolidin-1-ylsulfonyl)methyl]cyclobutyl}-7*H*-pyrrolo[2,3-*d*]pyrimidin-4-amine (43).** *Step 1:* Pyrrolidine (30 mg, 0.42 mmol) was added to a solution of **57b** (100 mg, 0.21 mmol) and DIPEA (0.18 mL, 1.0 mmol) in DCM (3 mL) at rt. The reaction mixture was stirred for 2 h at rt and then quenched with H_2O. The mixture was extracted with

EtOAc (20 mL). The organic layer was separated, washed with brine, and concentrated to afford crude *N*-methyl-*N*-{*cis*-3-[(pyrrolidin-1-ylsulfonyl)methyl]cyclobutyl}-7-[(4-methylphenyl)sulfonyl)]-7*H*-pyrrolo[2,3-*d*]pyrimidin-4-amine as a yellow oil, which was used in the following step without purification. LC/MS m/z (M + H^+) calcd for $C_{23}H_{30}N_5O_4S_2$: 504. Found: 504.

Step 2: K_2CO_3 (74 mg, 0.54 mmol) was added to a solution of crude *N*-methyl-*N*-{*cis*-3-[(pyrrolidin-1-ylsulfonyl)methyl]cyclobutyl}-7-[(4-methylphenyl)sulfonyl)]-7*H*-pyrrolo[2,3-*d*]pyrimidin-4-amine (90 mg, 0.18 mmol) in MeOH (3 mL) and THF (3 mL). The mixture was stirred at 50°C for 2 h and then quenched by addition of 1M aq. HCl solution (1 mL). The mixture was concentrated under vacuum and then purified by preparative HPLC (column: DuraShell 150 x 25mm x 5um; mobile phase: 23% MeCN to 43% MeCN in H_2O (0.05% NH_4OH) to afford the title compound as a white solid, 18.7 mg (30%). ^{1}H NMR (400 MHz, $CDCl_3$): 9.49 (br s, 1H), 8.33 (s, 1H), 7.08 (d, *J* = 3.7 Hz, 1H), 6.63 (d, *J* = 3.7 Hz, 1H), 5.11-5.20 (m, 1H), 3.39-3.44 (m, 4H), 3.38 (s, 3H), 3.16 (d, *J* = 7.0 Hz, 2H), 2.65-2.92 (m, 2H), 2.56-2.64 (m, 1H), 2.12-2.19 (m, 2H), 1.96-2.00 (m, 4H). LC/MS m/z (M + H^+) calcd for $C_{16}H_{24}N_5O_2S$: 350. Found: 350.

Benzyl [*cis*-3-(methylamino)cyclobutyl]carbamate hydrochloride and benzyl [*trans*-3-(methylamino)cyclobutyl]carbamate (*cis*-45·HCl and *trans*-45). A 2 M solution of methylamine in THF (825 mL, 1.65 mol) was slowly added to a mechanically stirred slurry of benzyl (3-oxocyclobutyl)carbamate (88 g, 0.40 mol) and AcOH (48.5 mL) at rt. The reaction mixture was stirred at rt for 2.5 h and then cooled to 0°C. $NaBH_4$ (49.5 g, 1.31 mol) was added in portions over 10 min. After addition was complete, the reaction mixture was allowed to warm to rt overnight. The reaction mixture was quenched with saturated aq. NH_4Cl solution (250 mL,

added slowly in portions of 25 mL) and then diluted with 5 M aq. NaOH solution until pH > 12. The mixture was extracted with MTBE (1500 mL). The organic layer was separated and washed with H_2O (250 mL) and brine (250 mL). Aqueous layers were back-extracted with MTBE (500 mL) and the combined MTBE layers were dried over $MgSO_4$, filtered and concentrated under vacuum to afford an oil. This was taken up in DCM (250 mL), concentrated again and re-dissolved in DCM (1100 mL). Anhydrous HCl gas was passed into the resulting solution at rt. The resulting slurry was concentrated under vacuum to afford the crude hydrochloride salt, which was recrystallized by dissolving in *i*-PrOH (1040 mL) at 70°C, adding heptane (260 mL), purging with additional HCl gas, and cooling to about 15°C. The solid (68.0 g, 63%) was collected by filtration, washing with 1:1 *i*-PrOH/heptane (250 mL) and drying under vacuum; HPLC analysis indicated the material to contain 98.4% benzyl [*cis*-3-(methylamino)cyclobutyl]carbamate hydrochloride and 1.6% benzyl [*trans*-3-(methylamino)cyclobutyl]carbamate hydrochloride. A second crop of material (18.9 g, 17%) containing 53% *cis* isomer and 47% *trans* isomer was subsequently obtained from the mother liquor. Small amounts of pure *trans* isomer were isolated by supercritical fluid chromatography on the free base mixture. *cis*-**45**·HCl: ^{1}H NMR: (400 MHz, D_2O): 7.30-7.34 (m, 5H); 5.00 (s, 2H), 3.80-3.88 (m, 1H), 3.31-3.40 (m, 1H), 2.61-2.70 (m, 2H), 2.52 (s, 3H), 1.95-2.05 (m, 2H). LC/MS m/z ($M + H^+$) calcd for $C_{13}H_{19}N_2O_2$: 235. Found: 235. *trans*-**45**: ^{1}H NMR (400 MHz, DMSO-d_6): 7.61 (br. d, J = 6.6 Hz, 1H), 7.29-7.42 (m, 5H), 5.01 (s, 2H), 4.22 (br s, 1H), 4.06-4.15 (m, 1H), 3.13-3.27 (m, 1H), 2.23 (s, 3H), 2.06-2.08 (m, 4H).

Benzyl [*cis*-3-(methyl{7-[(4-methylphenyl)sulfonyl]-7*H*-pyrrolo[2,3-*d*]pyrimidin-4-yl}amino)cyclobutyl]carbamate (47a). 4-Chloro-7-[(4-methylphenyl)sulfonyl]-7*H*-pyrrolo[2,3-*d*]pyrimidine (**46a**) (15 g, 48.7 mmol) and ***cis*-45**·HCl (17.2 g, 63.5 mmol) were mixed with *i*-

PrOH (180 mL) and DIPEA (28 mL, 161 mmol). The resulting slurry was heated at 75°C for 6 h. The reaction was cooled to rt, filtered, washed with *i*-PrOH (150 mL) and dried in an oven at 50°C to give the title compound (23.5 g, 95%) as a white solid. ^{1}H NMR (400 MHz, DMSO-d_6): 8.24 (s, 1H), 7.97 (d, J = 8.1 Hz, 2H), 7.62 (d, J = 4.0 Hz, 1H), 7.42 (d, J = 8.1 Hz, 2H), 7.29-7.40 (m, 6H), 6.98 (d, J = 4.0 Hz, 1H), 5.02 (s, 2H), 4.80-4.88 (m, 1H), 3.78-3.88 (m, 1H), 3.22 (s, 3H), 2.46-2.55 (m, 2H), 2.35 (s, 3H), 2.17-2.25 (m, 2H).

Benzyl{*cis*-3-[(2-chloro-7*H*-pyrrolo[2,3-*d*]pyrimidin-4-yl)(methyl)amino]-cyclobutyl}carbamate (47b). To a solution of K_2CO_3 (459.3 g, 3.32 mol) in H_2O (3 L) was added *cis*-**45**·HCl (225 g, 0.832 mol), followed by 2,4-dichloro-7*H*-pyrrolo[2,3-*d*]pyrimidine (**46b**) (156.4 g, 0.832 mol) at rt. After addition was complete, the reaction mixture was stirred at 95°C overnight. The mixture was filtered to collect the solid. The filter cake was washed with H_2O and dried under vacuum to afford the title compound (315 g, 98%) as a yellow solid. ^{1}H NMR (400 MHz, DMSO-d_6): 11.81 (br s, 1H), 7.63 (d, J = 8.2 Hz, 1H), 7.29-7.37 (m, 5H), 7.13 (d, J = 3.6 Hz, 1H), 6.64 (d, J = 3.6 Hz, 1H), 5.00 (s, 2H), 4.75-4.83 (m, 1H), 3.77-3.87 (m, 1H), 3.23 (s, 3H), 2.47-2.55 (m, 2H), 2.19-2.26 (m, 2H). LC/MS m/z (M + H^+) calcd for $C_{19}H_{21}ClN_5O_2$: 386. Found: 386.

***cis*-*N*-Methyl-N-{7-[(4-methylphenyl)sulfonyl]-7*H*-pyrrolo[2,3-*d*]pyrimidin-4-yl}cyclobutane-1,3-diamine dihydrobromide (48a·2HBr).** Compound **47a** (15.2 g, 30.1 mmol) was suspended in EtOAc (45 mL) and AcOH (45 mL). To the slurry was slowly added a 4M solution of HBr in AcOH (45 mL, 180 mmol), maintaining the temperature below 25°C. The resulting slurry was stirred at rt for 2 h. The solids were collected by filtration, washed with EtOAc (450 mL), and dried at 40°C to afford the title compound (16 g, 100%) as a white solid. ^{1}H NMR (400 MHz, MeOH-d_4): 8.43 (s, 1 H), 8.10 (d, J = 8.4 Hz, 2H), 7.89 (d, J = 4.1 Hz, 1H),

7.47 (d, J = 8.4 Hz, 2H), 7.21 (d, J = 4.1 Hz, 1H), 4.83-4.93 (m, 1H), 3.69-3.77 (m, 1H), 3.50 (s, 3 H), 2.86-2.93 (m, 2H), 2.58-2.67 (m, 2H), 2.45 (s, 3H). LC/MS m/z (M + H^+) calcd for $C_{18}H_{22}N_5O_2S$: 372. Found: 372. Anal. calcd for $C_{18}H_{23}Br_2N_5O_2S$: C, 40.54; H, 4.35; Br, 29.97; N, 13.13. Found: C, 40.10; H, 4.11; Br, 29.56; N, 12.86.

***cis*-*N*-Methyl-N-7*H*-pyrrolo[2,3-*d*]pyrimidin-4-ylcyclobutane-1,3-diamine hydrochloride (48b.HCl).** A mixture of **47b** (38.0 g, 98.4 mmol), $Pd(OH)_2$ (18.6 g, 119 mmol) and cyclohexene (212 mL, 2.08 mol) in EtOH (800 mL) was stirred at reflux for 3 h. The reaction mixture was filtered through a pad of diatomaceous earth washing with MeOH. The filtrate was concentrated under vacuum to afford the title compound (19 g, 76%) as a white solid. ^{1}H NMR (400 MHz, DMSO-d_6): 11.66 (br, 1H), 8.48 (br s, 3H), 8.09 (s, 1H), 7.14 (dd, J = 2.3, 3.7 Hz, 1H), 6.62 (dd, J = 1.9, 3.7 Hz, 1H), 5.06-5.15 (m, 1H), 3.43-3.51 (m, 1H), 3.31 (s, 3H) (remaining signals obscured by solvent). LC/MS m/z (M + H^+) calcd for $C_{11}H_{16}N_5$: 218. Found: 218.

***N*-[*cis*-3-(Methyl{7-[(4-methylphenyl)sulfonyl]-7*H*-pyrrolo[2,3-*d*]pyrimidin-4-yl}amino)cyclobutyl]-2-oxo-1,3-oxazolidine-3-sulfonamide (50).** To a solution of chlorosulfonyl isocyanate (1.76 mL, 20.6 mmol) in DCM (150 mL) was added dropwise a solution of 2-bromoethanol (1.43 mL, 20.6 mmol) in DCM (80 mL) at 0 °C. After 30 min at 0 °C, a solution of **48a**·2HBr (11.0 g, 20.6 mmol) and TEA (10.42 g, 103.2 mmol) in dry DCM (80 was added dropwise, and the reaction mixture was allowed to warm to rt overnight. The reaction solution was dissolved in DCM (1 L), washed with aq. 1M HCl solution (2 x 800 mL) and brine (500 mL). The solution was dried over Na_2SO_4 and concentrated to afford the title compound as white solid (8.5 g, 79%). ^{1}H NMR (400 MHz, DMSO-d_6): 8.83 (d, J = 9.4 Hz, 1H), 8.26 (s, 1H), 7.98 (d, J = 8.4 Hz, 2H), 7.66 (d, J = 4.1 Hz,1H), 7.44 (d, J = 8.4 Hz, 2H), 7.03 (d, J = 4.1 Hz, 1H), 4.80-4.88 (m, 1H), 4.38-4.41 (m, 2H), 3.95-3.99 (m, 2H), 3.63-3.73 (m,1H), 3.23 (s, 3H),

2.50-2.58 (m, 2H), 2.37 (s, 3H); 2.22-2.30 (m, 2H). LC/MS m/z ($M + H^+$) calcd for $C_{21}H_{25}N_6O_6S_2$: 521. Found: 521.

***cis*- and *trans*-[3-(Methylamino)cyclobutyl]methanol (53).** *Step 1:* di-*tert*-Butyl dicarbonate (15.8 g, 72.3 mmol) was added dropwise to a cold (0°C) solution of *cis*- and *trans*-**52** (*cis*/*trans* ~ 9:1)[36] (10 g, 55.7 mmol) and TEA (19.4 mL, 139.1 mmol) in DCM (370 mL). After addition was complete, the mixture was stirred at rt overnight. The solvent was evaporated under vacuum. The resulting residue was chromatographed eluting with a gradient of petroleum ether and ethyl acetate (10:1 to 3:1) to afford a ~9:1 mixture of *cis*- and *trans*-ethyl 3-[(tert-butoxycarbonyl)amino]cyclobutane carboxylate as a white solid (19 g, 92%). ^{1}H NMR (400 MHz, $CDCl_3$): 4.80 (br s, 1H), 4.12-4.18 (m, 3H), 2.72-2.81 (m, 1H), 2.60-2.63 (m, 2H), 2.06-2.14 (m, 2H), 1.45 (s, 9 H), 1.27 (t, J = 7.1 Hz, 3H).

Step 2: $LiAlH_4$ (9.14 g, 240.4 mmol) was suspended in dry THF (350 mL). The mixture was cooled to 0°C and a solution of ethyl 3-[(tert-butoxycarbonyl)amino]cyclobutane carboxylate (*cis*/*trans* ~ 9:1) (11.7 g, 48.1 mmol) in dry THF (170 mL) was added dropwise. After addition was complete, the resulting mixture was heated to reflux overnight. After it was cooled to rt, the reaction was diluted with THF (1.5 L) and then cooled to 0°C. Small portions of $Na_2SO_4.10\ H_2O$ were added until gas evolution had ceased. The mixture was filtered to remove the solids, which were washed with more THF (500 mL). The filtrate was concentrated to dryness affording the title mixture (cis/trans = 10:1) as an oil (10 g, >100%). ^{1}H NMR (400 MHz, MeOH-d_4): 3.60 (d, J = 7.0 Hz, 0.2H), 3.52 (d, J = 5.8 Hz, 1.8H), 3.15 (quin, J = 7.9 Hz, 0.9H), 2.28-2.42 (m, 1.8H), 2.34 (s, 3 H), 2.26-2.08 (m, 1.3H), 1.92-2.01 (m, 0.1H), 1.55-1.62 (m, 1.8 H).

***cis*-[3-(Methyl{7-[(4-methylphenyl)sulfonyl]-7*H*-pyrrolo[2,3-*d*]pyrimidin-4-yl}amino)cyclobutyl]methanol (54).** Potassium iodide (173 mg) and TEA (13 mL, 93.8 mmol) were added to a solution of *cis*/*trans*-**53** (6.0 g, 52.1 mmol) in acetone (250 mL). 4-Chloro-7-[(4-methylphenyl)sulfonyl]-7*H*-pyrrolo[2,3-*d*]pyrimidine (**46a**) (14.4 g, 46.8 mmol) was added and the resulting mixture was heated to reflux overnight. After evaporation of the solvent under reduced pressure, the residue was diluted with DCM (500 mL). The solution was washed sequentially with H_2O (300 mL), 2% aq. citric acid (300 mL) and brine (300 mL), and then dried over Na_2SO_4. After filtration, the solution was filtered and concentrated to afford the title mixture as a light solid (15.3 g, 85%). A portion (5.0 g) of the mixture was separated by supercritical fluid chromatography using a Chiralpak-AD column: *cis*-**54**: 4.6 g: ^{1}H NMR (400 MHz, DMSO-d_6): 8.23 (s, 1H), 7.97 (d, J = 8.2 Hz, 2H), 7.61 (d, J = 3.9 Hz, 1H), 7.42 (d, J = 8.2 Hz, 2H), 6.94 (d, J = 3.9 Hz, 1H), 4.96-5.05 (m, 1H), 4.58 (t, J = 5.3 Hz, 1H) 3.39-3.41 (m, 2H), 3.19 (s, 3H), 2.35 (s, 3H), 2.08-2.19 (m, 3H), 1.99-2.07 (m, 2H). LC/MS m/z (M + H^+) calcd for $C_{19}H_{23}N_4O_3S$: 387. Found: 387. In the ^{1}H NMR spectrum (400 MHz, DMSO-d_6) of the mixture of *cis*- and *trans*-**54** (before SFC), the latter isomer displayed distinct signals at 6.90 (d, J = 3.8 Hz, 1H), 5.19-5.27 (m, 1H), 4.69-4.73 (m, 1H), 3.50-3.53 (m, 2H), 3.23 (s, 3H).

***cis*-[3-(Methyl{7-[(4-methylphenyl)sulfonyl]-7*H*-pyrrolo[2,3-*d*]pyrimidin-4-yl}amino)cyclobutyl]methyl 4-methylbenzenesulfonate (55a).** To a solution of **54** (20 g, 51.8 mmol) and DMAP (12.6 g, 103.6 mmol) in DCM (500 mL) at 0°C was added *p*-toluenesulfonyl chloride (14.8 g, 77.7 mmol). The reaction mixture was stirred at rt for 16 h and then washed with H_2O (total 500 mL). The combined aqueous washes were extracted with DCM (2 x 800 mL). The combined organic layers were dried, filtered and concentrated under vacuum. The residue was chromatographed eluting with a gradient of 0% to 5% MeOH/DCM to afford the

title compound (23 g, 82%) as a white solid. ^{1}H NMR (400 MHz, DMSO-d_6): 8.23 (s, 1H), 7.97 (d, J = 8.0 Hz, 2H), 7.81 (d, J = 8.7 Hz, 2H), 7.62 (d, J = 3.9 Hz, 1H), 7.49 (d, J = 8.7 Hz, 2H), 7.44 (d, J = 8.0 Hz, 2H), 6.95 (d, J = 4.3 Hz, 1H), 4.95-5.03 (m, 1H), 4.10 (d, J = 6.2 Hz, 2H), 3.16 (s, 3H), 2.43 (s, 3H), 2.37 (s, 3H), 2.26-2.40 (m, 1H), 2.16-2.22 (m, 2H), 1.90-1.98 (m, 2H). LC/MS m/z (M + H^+) calcd for $C_{26}H_{29}N_4O_5S_2$: 541. Found: 541.

***cis*-[3-(Methyl{7-[(4-methylphenyl)sulfonyl]-7*H*-pyrrolo[2,3-*d*]pyrimidin-4-yl}amino)cyclobutyl]methyl methanesulfonate (55b).** To a solution of **54** (2.06 g, 5.3 mmol), TEA (2.25 mL, 16 mmol) and DMAP (33 mg, 0.23 mmol) in DCM (27 mL) at 0°C was added methanesulfonyl chloride (14.8 g, 77.7 mmol). The reaction mixture was stirred at 0°C for 2 h and then poured into saturated aq. $NaHCO_3$ solution. The resulting mixture was extracted three times with DCM. The combined organic layers were dried over $MgSO_4$, filtered and concentrated under vacuum. The residue was chromatographed eluting with a gradient of 5% to 100% EtOAc/heptane to afford the title compound (2.23 g, 90%) as a white solid. ^{1}H NMR (400 MHz, $CDCl_3$): 8.39 (s, 1H), 8.05 (d, J = 8.3 Hz, 2H), 7.47 (d, J = 4.0 Hz, 1H), 7.28 (d, J = 8.0 Hz, 2H), 6.64 (d, J = 4.0 Hz, 1H), 5.04-5.13 (m, 1H), 4.23 (d, J = 4.8 Hz, 2H), 3.24 (s, 3H), 3.03 (s, 3H), 2.39-2.46 (m, 3H), 2.38 (s, 3H), 2.05-2.13 (m, 2H). LC/MS m/z (M + H^+) calcd for $C_{20}H_{24}N_4O_5S_2$: 465. Found: 465.

***S*-{[*cis*-3-(Methyl{7-[(4-methylphenyl)sulfonyl]-7*H*-pyrrolo[2,3-*d*]pyrimidin-4-yl}amino)cyclobutyl]methyl} ethanethioate (56).** A solution of **55a** (2.0 g, 3.70 mmol) in DMF (6 mL) was added dropwise over 5 min to a solution of potassium thioacetate (678 mg, 5.93 mmol) in DMF (5 mL) at rt. The mixture was heated at 50-55°C overnight. The mixture was cooled to rt and quenched by pouring into saturated aq. $NaHCO_3$ solution (60 mL). The mixture was extracted with EtOAc (3 x 30 mL) and the combined organic layers were washed with H_2O

(3 x 30 mL), brine (30 mL). After drying over Na_2SO_4, the solution was concentrated. The residue was chromatographed eluting with a gradient of DCM and MeOH (100:0 to 80:20) to afford the title compound (1.2 g, 73%) as a yellow solid. ^{1}H NMR (400 MHz, DMSO-d_6): 8.24 (s, 1H), 7.97 (d, J = 7.7 Hz, 2H), 7.62 (d, J = 3.9 Hz, 1H), 7.44 (d, J = 8.2 Hz, 2H), 6.96 (d, J = 4.3 Hz, 1H), 4.88-4.96 (m, 1H), 3.20 (s, 3H), 3.02 (d, J = 7.0 Hz, 2H), 2.37 (s, 3H), 2.35 (s, 3H), 2.26-2.33 (m, 2H), 2.13-2.24 (m, 1H), 1.87-1.92 (m, 2H). LC/MS m/z (M + H^+) calcd for $C_{21}H_{25}N_4O_3S_2$: 445. Found: 445.

[*cis*-3-(Methyl{7-[(4-methylphenyl)sulfonyl]-7*H*-pyrrolo[2,3-*d*]pyrimidin-4-yl}amino)cyclobutyl]methanesulfonic acid (57a). To a solution of **56** (580 mg, 1.30 mmol) in formic acid (10 mL) at rt was added 30% aq. H_2O_2 solution (0.7 mL, 6.9 mmol). The resulting mixture was stirred at rt overnight. The reaction was poured into 33% aq. $Na_2S_2O_5$ solution (1.1 mL) and then stirred for 10 min. Aqueous 33% NaOH solution (1.8 mL) was then added to adjust the pH to 5. The resulting mixture was stirred at rt for 1 h. The solid was collected by filtration, washed with H_2O (10 mL) and vacuum dried at about 60°C to afford the title compound (634 mg, crude) as a white solid. ^{1}H NMR (400 MHz, DMSO-d_6): 8.24 (s, 1H), 7.97 (d, J = 8.4 Hz, 2H), 7.62 (d, J = 4.2 Hz, 1H), 7.43 (d, J = 8.4 Hz, 2H), 6.96 (d, J = 4.2 Hz, 1H), 4.85-4.90 (m, 1H), 3.20 (s, 3H), 2.60-2.62 (m, 2H), 2.36 (s, 3H), 2.35-2.30 (m, 3H), 1.98-2.02 (m, 2H). LC/MS m/z (M + H^+) calcd for $C_{19}H_{23}N_4O_5S_2$: 451. Found: 451.

***cis*-[3-(Methyl{7-[(4-methylphenyl)sulfonyl]-7*H*-pyrrolo[2,3-*d*]pyrimidin-4-yl}amino)cyclobutyl]methanesulfonyl chloride (57b).** Thionyl chloride (0.3 mL, 3.33 mmol) was added dropwise over 5 min to a solution of **57a** (150 mg, 0.33 mmol) in DCM (20 mL) at 0°C. Two drops of DMF were added to the solution, which was then heated at 75°C for 2 h. The mixture was cooled and the solvent was evaporated. The residue was washed with anhydrous

DCM (3 x 10 mL) to afford the crude title compound (170 mg) as a yellow solid. LC/MS m/z (M + H^+) calcd for $C_{19}H_{22}ClN_4O_4S_2$: 469. Found: 469.

Caliper JAK enzyme endpoint IC_{50} assays at 1mM ATP:

Sample preparation: Test compounds were solubilized in DMSO to a stock concentration of 30 mM. Compounds were diluted in DMSO to create an 11-point half log dilution series with a top concentration of 600 μM. The test compound plate also contained positive control wells with a known inhibitor to define 100% inhibition and negative control wells with DMSO to define no inhibition. The compound plates were diluted 1 to 60 in the assay, resulting in a final assay compound concentration range of 10 μM to 100 pM and a 1.7% DMSO concentration.

The human JAK activity of was determined by using a microfluidic assay to monitor phosphorylation of a synthetic peptide by the recombinant human kinase domain of each of the four members of the JAK family, JAK1, JAK2, JAK3 and TYK2. Each assay condition was optimized for enzyme concentration and room temperature incubation time to obtain a conversion rate of 20% - 30% phosphorylated peptide product. 250 nL of test compounds and controls solubilized in 100% DMSO were added to a 384 well polypropylene plate (MatricalMP101 or Corning Costar 3676) using an non-contact acoustic dispenser. Kinase assays were carried out at room temperature in a 15 μL reaction buffer containing 20 mM HEPES, pH 7.4, 1mM ATP, 10 mM magnesium chloride, 0.01% bovine serum albumin (BSA), 0.0005% Tween 20 and 1mM DTT. Reaction mixtures contained 1 μM of a fluorescently labeled synthetic peptide, a concentration less than the apparent K_m. The JAK1 and TYK2 assays contained 1 μM of the peptide 5FAM-KKSRGDYMTMQID and the JAK2 and JAK3 assays contained 1 μM of the peptide FITC-KGGEEEEYFELVKK. The assays were initiated

by the addition of enzyme. The assays were stopped with 15 μL of a buffer containing 180 mM HEPES, pH = 7.4, 20 mM EDTA, 0.2% Coating Reagent, resulting in a final concentration of 10 mM EDTA, 0.1% Coating Reagent and 100 mM HEPES, pH = 7.4. Utilizing the LabChip® 3000 mobility shift technology (Caliper Life Science), each assay reaction was sampled to determine the level of phosphorylation. This technology is separation-based, allowing direct detection of fluorescently labeled substrates and products. Separations are controlled by a combination of vacuum pressure and electric field strength optimized for each peptide substrate.

Human Whole Blood (HWB) assays: Test articles were prepared as 30 mM stocks in 100% DMSO, and then diluted to 5 mM. A 10-point 2.5 dilution series was created in DMSO with a top concentration of 5 mM. Further dilution was done by adding 4 μL of the above test article solutions into 96 μL of PBS with a top concentration of 200 μM.

Cytokines IL-6 (cat. no. 206-IL), IL-10 (cat. no. 217-IL), IL-12 (cat. no. 219-IL), IL-15 (cat. no. 247-IL), IL-23 (cat. no. 1290-IL), IL-27 (cat. no. 2526-IL), IFNα (cat. no. 11200-2), IFNγ (cat. no. 285-IF) and EPO (cat no. 287 TC) were obtained from R&D Systems (Minneapolis, MN). IL-21 (cat. no. AF-200-21) was purchased from PeproTech (Rocky Hill, NJ). Antibodies specific to pSTATs and CDs were supplied by BD Biosciences (San Jose, CA); Anti-pSTAT1-AlexaFluor647, cat. no. 612597; Anti-pSTAT3-AlexaFluor647, cat. no. 557815; Anti-pSTAT4-AlexaFluor647, cat. no. 558137; Anti-pSTAT5-AlexaFluor647, cat. no. 612599; anti-CD3-Pacific Blue, cat. no. 558117; anti-CD14-Pacific Blue, cat. no. 558121. Phosflow 5x Lyse/Fix Buffer (cat. no. 558049) was purchased from BD Biosciences. Bovine serum albumin (BSA, 30% sterile solution; cat. no. A8327) and sodium azide (cat. no. S8032) were received from Sigma Aldrich. D-PBS (without Ca^{+2} or Mg^{+2}) was from Invitrogen (cat. no. 14190; Grand Island, NY).

Cryopreserved human bone marrow $CD34^+$ cells (cat. no. ABM022F) were purchased from Allcells. Frozen bone marrow $CD34^+$ cells were thawed, washed once with IMEM, re-suspended in Stem Span medium (cat. no. 09600; STEMCELL Technologies, Vancouver, Canada) supplemented with 20 ug/mL of LDL (cat. no. 02698; STEMCELL Technologies), 100 ng/mL Kit Ligand (cat. no. 255 SC; R&D Systems), and 2 U/mL EPO at 20,000 cells/mL and cultured for 7 days. $CD34^+$ cells were then harvested, washed once with D-PBS, and re-suspended at 0.5 million cells/mL in HWB to be used in the EPO stimulation assay.

To a 96-well polypropylene plate (VWR cat. no. 82007-292) 90 µl of HWB was added per well, followed by addition of 5 µl test article solutions prepared above to give a top concentration of 10 µM. The plate was mixed and incubated for 45 min at 37ºC. To each well was added 5 µl of cytokine (5 uL/well; final, 5000 U/mL IFNα, 100 ng/mL IFNγ, 50 ng/mL IL-6, 30 ng/mL IL-10, 5 ng/mL IL-12, 30 ng/mL IL-15, 50 ng/mL IL-21, 100 ng/mL IL-23, 1200 ng/mL IL-27 or 2 U/mL EPO) for 15 min. Anti-CD3-Pacific Blue and anti-CD14-Pacific Blue antibodies (1 to 6 dilution in D-PBS, 3 uL/well) were added to samples 15 min before the stimulation of IL-6 and IFNγ, respectively. The reaction was quenched by adding Lyse/Fix Buffer to all wells at 1000 µL/well and incubated for 20 min at 37ºC; after washing with FACS buffer [D-PBS containing 0.1 % BSA and 0.1% sodium azide], 400 µL ice cold 90% MeOH/H_2O was added to each well and incubated on ice for 30 min. One more wash was done with cold FACS buffer and all samples were finally resuspended in 250 µL/well of the desired Alexa Fluor 647 conjugated anti-phospho-STAT antibodies at 1:125 dilution in FACS buffer. Anti-pSTAT1-AlexaFluor647 was used in assays with stimulation from IFNγ and IL-6. Anti-pSTAT3-AlexaFluor647 was used in assays with stimulation from IFNα, IL-6, IL-10, IL-21, IL-23 and IL-27. Anti-pSTAT4-AlexaFluor647 was used in assays with stimulation from IL-12.

Anti-pSTAT5-AlexaFluor647 was used for IL-15 and EPO stimulated cells. After overnight incubation at 4° C all the samples were transferred into a 96-well polypropylene U-bottom plate (Falcon cat. no. 353077) and flow cytometric analysis was performed on a FACSCalibur™, FACSCanto™ or LSRFortessa™ equipped with a HTS plate loader (BD Biosciences). For IL-10, IL-12, IL-15, IL-21, IL-23, IL-27 and IFNα stimulation, the lymphocyte population was gated for histogram analysis of pSTAT3, 4 or 5 staining. For EPO stimulation, all events (entire populations) were gated for histogram analysis of pSTAT5 staining. For IFNγ stimulation, $CD14^+$ cells were gated for histogram analysis of pSTAT1 staining. For IL-6 stimulation, $CD3^+$ cells were gated for histogram analysis of pSTAT1 and 3 staining. Background fluorescence was defined using unstimulated cells and a gate was placed at the foot of the peak to include ~0.5% gated population. The histogram statistical analysis was performed using CellQuest™ Pro version 5.2.1 (BD Biosciences), FACSDiva™ version 6.2 (BD Biosciences) or FlowJo® version 7.6.1 (Ashland, OR) software. Relative fluorescence unit (RFU), which measures the level of phospho STAT, was calculated by multiplying the percent positive population and its mean fluorescence. Data from 10 compound concentrations (singlicate at each concentration) was normalized as a percentage of control based on the formula:

$$\% \text{ of Control} = 100 \times (A-B)/(C-B)$$

Where A is the RFU from wells containing compound and cytokine, B is the RFU from wells without cytokine (minimum fluorescence) and C is the RFU from wells containing only cytokine (maximum fluorescence). Inhibition curves and IC_{50} values were determined using the Prism version 5 software (GraphPad, La Jolla, CA).

Rat pharmacology studies

A) Rat WB stimulation and flow cytometry: Seventy μL of rat WB was surface stained with Anti-CD3-PE (eBiosciences cat. no. 12-0030-82) and rat anti-mouse CD4-FITC (BD Biosciences cat. no. 554843) for 15 min at 37°C. Rat whole blood was then stimulated with either 100ng/mL rmIL-21 (R&D Systems cat. no. 594-ML), 100ng/mL rhIL6 (R&D Systems cat. co. 206-IL) or 100ng/mL of rrIFNγ (R&D Systems cat. no. 585-IF) for 20 min at 37°C. Following incubation RBCs were lysed using BD Phosflow™ Lyse/Fix buffer (BD Biosciences cat. no. 558049) and cells subsequently permeabilized at 4°C using 90% MeOH. Cells were washed twice in FACS buffer and stained using Alexa Fluor 647 conjugated anti-phospho-STAT1 (PY701, BD Biosciences, cat. no. 612597) or anti-phospho STAT3 (PY705, BD Biosciences, cat. co. 557815). Flow cytometry was performed using a FACS LSR Fortessa (BD Biosciences). FlowJo® software version 7.6.1 was used for data analysis (Tree Star Inc., Ashland, OR). Intracellular STAT3 and STAT1 phosphorylation was determined within a CD3+ gate representing the T cell population. The level of STAT phosphorylation observed in whole blood from vehicle treated rats was referenced as the maximal response to cytokine stimulation. Data was normalized as a percent of vehicle treated animals using the following formula:

$$\% \text{ of vehicle} = (A-B)/(C-B)$$

A is experimental mean fluorescence, B is background fluorescence determined from unstimulated cells and C is maximum fluorescence determined by vehicle treated animals. Graphs were generated using Prism Graph Pad version 6 (La Jolla, CA).

B) Rat adjuvant induced arthritis model: The effect of JAK1 inhibition by **25** was evaluated in vivo using a therapeutic dosing paradigm in a rat adjuvant-induced arthritis. The efficacy of this molecule was evaluated in two separate studies using successively lower doses. Arthritis was

induced by immunization of female Lewis rats (8 to 10 weeks old; Charles River Laboratories, Portage, MI) via intradermal injection at the base of the tail with complete Freund's adjuvant with three 50 μL injections (15 mg/mL Mycobacterium tuberculosis (Difco) in incomplete Freund's adjuvant (Sigma Aldrich). Seven days after the initial immunization, the baseline hind paw volume of the immunized rats was measured via plethysmograph (Buxco Inc.). The rats were monitored daily for signs of arthritis including change in body weight and hind paw volume measurement. When individual hind paw volume measurements indicated an increase of 0.2 mL (or greater) in a single hind paw, animals were randomly assigned to a treatment group. Daily treatment with **25** was administered via oral gavage. Treatment groups for Experiment 1 were: 50, 15 and 5 mg/kg or vehicle (2% Tween 80 /0.5% methylcellulose/deionized H_2O). Treatment groups for Experiment 2 were: 15, 5, 1, and 0.5 mg/kg or vehicle (2% Tween 80 /0.5% methylcellulose/deionized H_2O). Dosing began once individuals were enrolled into respective groups. Treatment continued for 7 days. Animals were euthanized after 7 days of dosing. At the conclusion of the study, whole blood was taken at 15 min post-dose (peak concentration in plasma) for analysis of STAT phosphorylation and plasma was taken at peak (0.25 h) and trough (24 h) time points for exposure PK.

All activities involving laboratory animals were carried out in accordance with federal, state, local and institutional guidelines governing the use of laboratory animals in research and were reviewed and approved by Pfizer (or other) Institutional Animal Care and Use Committee. Pfizer animal care facilities that supported this work are fully accredited by AAALAC International.

ASSOCIATED CONTENT

Supporting information

The material is available free of charge via the internet at http://pubs.acs.org.

Inhibition values for JAK3,TYK2 and permeability measured using RRCK, fraction unbound compared to LogD, kinase selectivity table for **25,** Initial range finding rAIA study with **25** at doses of 5, 15, and 50 mpk, cytokine inhibition values in HWB for **19**, **25**, **35**, and **36**.

Molecular formula strings (CSV)

PDB ID code

Atomic coordinates for the x-ray structure of compound **25** in JAK1 and JAK2 can be accessed using PDB code 6BBU and 6BBV respectively in the RCSB Protein Data Bank (www.rcsb.org). Authors will release the atomic coordinates upon article publication.

AUTHOR INFORMATION

Corresponding authors

Ray Unwalla: Phone: 617-674-7398. E-mail: ray.unwalla@pfizer.com

Ralph P. Robinson: Phone: 860-441-4923. E-mail: ralph.p.robinson@pfizer.com

ORCID

Michael L. Vazquez : 0000-0001-6244-6540

Ray Unwalla : 0000-0002-5789-7336

Ralph P. Robinson : 0000-0002-4066-5299

Notes

The authors were all employees of Pfizer while this work was completed and declare no competing interests.

ACKNOWLEDGEMENTS

Michael Vazquez was the project leader during the discovery of PF-04965842. We thank Karen Coffman, Chris Dehnhardt, Shane Eisenbeis, Steve Kortum, Matthew Reese, Derek Sheehan and Jamison Tuttle for their contributions to analog synthesis, resynthesis and characterization. We thank Blossom Sneed for running the JAK caliper assays.

ABBREVIATIONS USED

AcOH, acetic acid; $(Boc)_2O$, di-*tert*-butyl dicarbonate; DBU, 1,8-diazabicycloundec-7-ene; DCE, 1,2-dichloroethane; DCM, dichloromethane; DIPEA, diisopropylethylamine; DMAP, 4-dimethylaminopyridine; DMF, *N*,*N*-dimethylformamide; DMSO, dimethylsulfoxide; DTT, dithiothreitol; EtOAc, ethyl acetate; EtOH, ethanol; h, hour; *i*-PrOH, isopropyl alcohol; LiHDMS, lithium hexamethyldisilazide; MeOH, methanol; MeCN, acetonitrile; MTBE, methyl *tert*-butyl ether; min, minute; NMP, *N*-methylpyrrolidinone; PK, pharmacokinetics; rt, room temperature; RRCK, Ralph Russ canine kidney; TEA, triethylamine; TBAF, tetrabutylammonium fluoride; THF, tetrahydrofuran.

REFERENCES

1. (a) Leonard, W. J.; O'Shea, J. J. JAKS and STATS: biological implications. *Annu. Rev. Immunol*. **1998**, *16*, 293−322. (b) Ghoreschi, K.; Laurence, A.; O'Shea, J. J. Janus kinases in immune cell signaling. *Immunol. Rev.* **2009**, *228*, 273−287. (c) Johnston, J. A.; Bacon, C. M.; Riedy, M. C.; O'Shea, J. J. Signaling by IL-2 and related cytokines: JAKs, STATs, and relationship to immunodeficiency. *J. Leukocyte Biol.* **1996**, *60*, 441−452. (d) O'Shea, J. J.; Plenge, R. JAK and STAT signaling molecules in immunoregulation and immune-mediated disease. *Immunity* **2012**, *36*, 542−550. (e) Shuai, K.; Liu, B. Regulation of JAK-STAT signaling in the immune system. *Nat. Rev. Immunol.* **2003**, *3*, 900−911.
2. Mavers, M.; Ruderman, E. M.; Perlman, H. Intracellular signal pathways: potential for therapies. *Curr. Rheumatol. Rep*. **2009**, *11*, 378−385.
3. Schindler, C.; Levy, D. E.; Decker, T. JAK-STAT Signaling: from interferons to cytokines. *J. Biol. Chem.* **2007**, *282*, 20059−20063.
4. Hofmann, S. R.; Ettinger, R.; Zhou, Y.-J.; Gadina, M.; Lipsky, P.; Siegel, R.; Candotti, F.; O'Shea, J. J. Cytokines and their role in lymphoid development, differentiation and homeostasis. *Curr. Opin. Allergy Clin. Immunol.* **2002**, *2,* 495−506.
5. Levy, D. E.; Darnell, J. E., Jr. STATS: Transcriptional control and biological impact. *Nat. Rev. Mol. Cell Biol.* **2002**, *3*, 651−662.
6. Rodig, S. J.; Meraz, M. A.; White, J. M.; Lampe, P. A.; Riley, J. K.; Arthur, C. D.; King, K. L.; Sheehan, K. C. F.; Yin, L.; Pennica, D.; Johnson, E. M., Jr.; Schreiber, R. D. Disruption of the Jak1 gene demonstrates obligatory and nonredundant roles of the JAKs in cytokine-induced biologic responses. *Cell* **1998,** *93,* 373–383.

7. Kaur, K.; Kalra, S.; Kaushal, S. Systematic Review of Tofacitinib: A new drug for the management of rheumatoid arthritis. *Clin. Therapeutic* **2014**, *36*, 1074-1086.
8. Fridman, J. S.; Scherle, P. A.; Collins, R.; Burn, T. C.; Li, Y.; Li, J.; Covington, M. B.; Thomas, B.; Collier, P.; Favata, M. F.; Wen, X.; Shi, J.; McGee, R.; Haley, P. J.; Shepard, S.; Rodgers, J. D.; Yeleswaram, S.; Hollis, G.; Newton, R. C.; Metcalf, B.; Friedman, S M.; Vaddi, K. Selective inhibition of JAK1 and JAK2 is efficacious in rodent models of arthritis: preclinical characterization of INCB028050. *J. Immunol.* **2010,** *184,* 5298−5307.
9. Mesa, R. A.; Yasothan, U.; Kirkpatrick, P. Ruxolitinib. *Nat. Rev. Drug Discovery* **2012**, *11*, 103−104.
10. Schwartz, D.; Bonelli, M.; Gadina, M.; O'Shea, J. Type 1/11 cytokines, JAKs, and new design strategies for treating autoimmune diseases, *Nat. Rev. Rheumatol.* **2016**, *12*, 25-36. Keystone E. C.; Taylor, P.; Drescher, E.; Schlichting, D.; Beattie, D.; Berclaz, P.; Lee, C.; Fidelus-Gort, R.; Luchi, M.; Rooney, T.; Macias, W.; Genovese, M. Safety and efficacy of baricitinib at 24 weeks in patients with rheumatoid arthritis who have an inadequate response to methotrexate. *Ann. Rheum. Dis.* **2015**, *74*, 333–340.
11. Strober, B.; Buonanno, M.; Clark, J. D.; Kawabata, T.; Tan, H.; Wolk, R.; Valdez, H.; Langley, R. G.; Harness, J.; Menter, A.; Papp, K. Effect of tofacitinib, a Janus kinase inhibitor, on haematological parameters during 12 weeks of psoriasis treatment. *Br. J. Dermat.* **2013**, *169*, 992–999.
12. Noguchi, M.; Yi, H.; Rosenblatt, H. M.; Filipovich, A. H.; Adelstein, S.; Modi, W. S.; McBride, O. W.; Leonard, W. J. Interleukin-2 receptor gamma chain mutation results in X-linked severe combined immunodeficiency in humans. *Cell* **1993**, *73*, 147−157.

13. Changelian, P. S.; Flanagan, M. E.; Ball, D. J.; Kent, C. R.; Magnuson, K. S.; Martin, W. H.; Rizzuti, B. J.; Sawyer, P. S.; Perry, B. D.; Brissette, W. H.; McCurdy, S. P.; Kudlacz, E. M.; Conklyn, M. J.; Elliott, E. A.; Koslov, E. R.; Fisher, M. B.; Strelevitz, T. J.; Yoon, K.; Whipple, D. A.; Sun, J.; Munchhof, M. J.; Doty, J. L.; Casavant, J. M.; Blumenkopf, T. A.; Hines, M.; Brown, M. F.; Lillie, B. M.; Subramanyam, C.; Shang-Poa, C.; Milici, A. J.; Beckius, G. E.; Moyer, J. D.; Su, C.; Woodworth, T. G.; Gaweco, A. S.; Beals, C. R.; Littman, B. H.; Fisher, D. A.; Smith, J. F.; Zagouras, P.; Magna, H. A.; Saltarelli, M. J.; Johnson, K. S.; Nelms, L. F.; Des Etages, S. G.; Hayes, L. S.; Kawabata, T. T.; Finco-Kent, D.; Baker, D. L.; Larson, M.; Si, M. S.; Paniagua, R.; Higgins, J.; Holm, B.; Reitz, B.; Zhou, Y. J.; Morris, R. E.; O'Shea, J. J.; Borie, D. C. Prevention of organ allograft rejection by a specific Janus kinase 3 inhibitor. *Science* **2003**, *302*, 875–878.

14. Clark, J. D.; Flanagan, M. E; Telliez, J-B. Discovery and development of Janus kinase (JAK) inhibitors for inflammatory diseases. *J. Med. Chem.* **2014**, *57*, 5023–5038.

15. Flanagan, M. E.; Blumenkopf, T. A.; Brissette, W. H.; Brown, M. F.; Casavant, J. M.; Chang, S.-P.; Doty, J. L.; Elliott, E. A.; Fisher, M. B.; Hines, M.; Kent, C.; Kudlacz, E. M.; Lillie, B. M.; Magnuson, K. S.; McCurdy, S. P.; Munchhof, M. J.; Perry, B. D.; Sawyer, P. S.; Strelevitz, T. J.; Subramanyam, C.; Sun, J.; Whipple, D. A.; Changelian, P. S. Discovery of CP-690,550: a potent and selective Janus kinase (JAK) inhibitor for the treatment of autoimmune diseases and organ transplant rejection. *J. Med. Chem.* **2010**, *53*, 8468−8484.

16. Meyer, D. M.; Jesson, M. I.; Li, X.; Elrick, M. M.; Funckes-Shippy, C. L.; Warner, J. D.; Gross, C. J.; Dowty, M. E.; Ramaiah, S. K.; Hirsch, J. L.; Sabbye, M. J.; Barks, J. L.;

Kishore, N.; Morris, D. L. Anti-inflammatory activity and neutrophil reductions mediated by the JAK1/JAK3 inhibitor, CP-690,550, in rat adjuvant-induced arthritis. *J. Inflamm.* **2010**, *7*, 41.

17. a) Menet, C. J.; Van Rompaey, L.; Geney, R. Advances in the discovery of selective JAK inhibitors. *Prog. Med. Chem*. **2013,** *52*, 153–223. b) Menet, C.; Mammoliti, O.; Lopez-Ramos, M. Progress toward JAK1-selective inhibitors. *Future Med. Chem.* **2015,** *7,* 203-235.

18. a) Thorarensen, A.; Banker, M. E.; Fensome, A.; Telliez, J-B.; Juba, B.; Vincent, F.; Czerwinski, R. M.; Casimiro-Garcia, A. ATP mediated kinome selectivity – The missing link in understanding the contribution of individual JAK kinases isoforms to cellular signaling. *ACS Chemical Biology* **2014**, *9*, 1552–1558. b) Cheng, Y., and Prusoff, W. H. Relationship between the inhibition constant (KI) and the concentration of inhibitor which causes 50% inhibition (I50) of an enzymatic reaction. *Biochem. Pharmacol.* **1973**, *22***,** 3099−4108.

19. Kremer, J. M.; Cohen, S.; Wilkinson, B. E.; Connell, C. A.; French, J. L.; Gomez-Reino, J.; Gruben, D.; Kanik, K. S.; Krishnaswami, S.; Pascuala-Ramos, V.; Wallenstein, G.; Zwillich, S. H. A phase 2B dose-ranging study of the oral JAK inhibitor tofacitinib (CP-690,550) versus placebo in combination with background methotrexate in patients with active rheumatoid arthritis and inadequate response to methotrexate alone. *Arthritis Rheum.* **2012**, *64*, 970−981.

20. a) Di, Li.; Keefer, C.; Scott, Dennis.; Strelevitz, T.; Chang, G.; Bi, Yi-An.; Lai, Y.; Duckworth, J.; Fenner, K.; Troutman, M.; Obach, S.; Mechanistics insights from comparing intrinsic clearance values between human liver microsomes and hepatocytes

to guide drug design. Eur. J. of Med. Chem. **2012**, *57*, 441-448. (b) Chrencik, J. E.; Patny, A.; Leung, I. K.; Korniski, B.; Emmons, T. L.; Hall, T.; Weinberg, R. A.; Gormley, J. A.; Williams, J. M.; Day, J. E.; Hirsch, J. L.; Kiefer, J. R.; Leone, J. W.; Fischer, H. D.; Sommers, C. D.; Huang, H-C.; Jacobsen, E. J.; Tenbrink, R. E.; Tomasselli, A. G.; Benson, T. E. Structural and thermodynamic characterization of the TYK2 and JAK3 kinase domains in complex with CP-690550 and CMP-6. *J. Mol. Biol.* **2010**, *400*, 413–433.

21. a) Andrews, P. R.; Craik, D. J.; Martin, J. L. Functional group contributions to drug-receptor interactions. *J. Med. Chem.* **1984**, *27*, 1648-1657. b) Schonherr, H.; Cernak, T. Profound methyl effects in drug discovery and a call for new methylation reactions. *Angew. Chem. Int. Ed*. **2013**, *52*, 12256-12267.
22. Caspers, N.; Han, S.; Rajamohan, F.; Hoth, L.; Geoghegan, K.; Subashi, T.; Knafels, J.; Vazquez, M.; Kaila, N.; Cronin, C.; Johnson, E.; Kurumbail, R. Development of a high-throughput crystal structure-determination platform for JAK1 using a novel metal-chelator soaking system. *Acta Crystallogr., Sect. F: Struc. Biol. Commun*. **2016**, *72*, 840-845.
23. Williams, N. K.; Bamert, R. S.; Patel, O.; Wang, C.; Walden, P. M.; Wilks, A. F.; Fantino, E.; Rossjohn, J.; Lucet, I. S. Dissecting specificity in the Janus kinases: The structures of JAK-specific inhibitors complexed to the JAK1 and JAK2 protein tyrosine kinase domains. *J. Mol. Biol.* **2009***, 387*, 219-232.
24. (a) Zak, M.; Hurley, C. A.; Ward, S. I.; Bergeron, P.; Barrett, K.; Balazs, M.; Blair, W. S.; Bull, R.; Chakravarty, P.; Chang, C.; Crackett, P.; Deshmukh, G.; DeVoss, J.; Dragovich, P. S.; Eigenbrot, C.; Ellwood, C.; Gaines, S.; Ghilardi, N.; Gibbons, P.;

Gradl, S.; Gribling, P.; Hamman, C.; Harstad, E.; Hewitt, P.; Johnson, A.; Johnson, T.; Kenny, J. R.; Koehler, M. F. T.; Bir Kohli, P.; Labadie, S.; Lee, W. P.; Liao, J.; Liimatta, M.; Mendonca, R.; Narukulla, R.; Pulk, R.; Reeve, A.; Savage, S.; Shia, S.; Steffek, M.; Ubhayakar, S.; van, A. A.; Aliagas, I.; Avitabile-Woo, B.; Xiao, Y.; Yang, J.; Kulagowski, J. J. Identification of C-2 hydroxyethyl imidazopyrrolopyridines as potent JAK1 inhibitors with favorable physicochemical properties and high selectivity over JAK2. *J. Med. Chem.* **2013**, *56*, 4764−4785.(b) Labadie, S.; Dragovich, P. S.; Barrett, K.; Blair, W. S.; Bergeron, P.; Chang, C.; Deshmukh, G.; Eigenbrot, C.; Ghilardi, N.; Gibbons, P.; Hurley, C. A.; Johnson, A.; Kenny, J. R.; Bir Kohli, P.; Kulagowski, J. J.; Liimatta, M.; Lupardus, P. L.; Mendonca, R.; Murray, J. M.; Pulk, R.; Shia, S.; Steffek, M.; Ubhayakar, S.; Ultsch, M.; van Abbema, A.; Ward, S.; Zak, M. Structure-based discovery of C-2 substituted imidazo-pyrrolopyridine JAK1 inhibitors with improved selectivity over JAK2. *Bioorg. Med. Chem. Lett.* **2012,** *22,* 7627-7633.

25. (a) Vasbinder, M. M.; Alimzhanov, M.; Augustin, M.; Bebernitz, G.; Bell, K.; Chuaqui, C.; Deegan, T.; Ferguson, A. D.; Goodwin, K.; Huszar, D.; Kawatkar, A.; Kawatkar, S.; Read, J.; Shi, J.; Steinbacher, S.; Steuber, H.; Su, Q.; Toader, D.; Wang, H.; Woessner, R.; Wu, A.; Ye, M.; Zinda, M. Identification of azabenzimidazoles as potent JAK1 selective inhibitors. *Bioorg. Med. Chem. Lett.* **2016**, *26*, 60–67. (b) Simov, V.; Deshmukh, S. V.; Dinsmore, C. J.; Elwood, F.; Fernandez, R. B.; Garcia, Y.; Gibeau, C.; Gunaydin, H.; Jung, J.; Katz, J. D.; Kraybill, B.; Lapointe, B.; Patel, S. B.; Siu, T.; Su, H.; Young, J. R. Structure-based design and development of (benz)imidazole pyridones as JAK1-selective kinase inhibitors. *Bioorg. Med. Chem. Lett.* **2016**, *26*, 1803–1808.

26. (a) Allen, F. H.; Taylor, R. Research applications of the Cambridge Structural Database (CSD). *Chem. Soc. Rev*. **2004**, *33*, 463-475. (b) CCDC Website database: http://www.ccdc.cam.ac.uk/free_services/website/, acccessed on December 9, 2017.

27. Brameld, K. A.; Kuhn, B.; Reuter, D. C.; Stahl, M. Small molecule conformational preferences derived from crystal structure data. A medicinal chemistry focused analysis. *J. Chem. Inf. Model.* **2008,** *48,* 1-24.

28. Kulagowski, J. J.; Blair, W.; Bull, R. J.; Chang, C.; Deshmukh, G.; Dyke, H. J.; Eigenbrot, C.; Ghilardi, N.; Gibbons, P.; Harrison, T. K.; Hewitt, P. R.; Liimatta, M.; Hurley, C. A.; Johnson, A.; Johnson, T.; Kenny, J. R.; Bir, K. P.; Maxey, R. J.; Mendonca, R.; Mortara, K.; Murray, J.; Narukulla, R.; Shia, S.; Steffek, M.; Ubhayakar, S.; Ultsch, M.; vanAbbema, A.; Ward, S. I.; Waszkowycz, B.; Zak, M. Identification of imidazo-pyrrolopyridines as novel and potent JAK1 inhibitors. *J. Med. Chem.* **2012**, *55*, 5901−5921.

29. PetaChem, LLC, 26040 Elena Road, Los Altos Hills, CA 94022. Conformational Analysis: All quantum mechanical calculations were performed with the PetaChem software utilizing the B3LYP density functional with the 6-31G++ basis set in gas phase. Dihedral scans were performed using a series of constrained optimizations, whereby the specified dihedral angle was kept frozen at a given value, with full optimization of the remaining geometric parameters subject to the given dihedral constraint. Total energies for a given system were then converted into relative energies (kcal/mol) for graphical depiction.

30. This dihedral value is dependent on the pyramidalisation of the nitrogen in small molecule X-ray structures. Sulfonamide nitrogen atoms are generally depicted as slightly less pyramidal with an N-plane distance between 0.25-0.4 Å but often lower.
31. a) Hegen, M.; Keith, Jr, J.; Collins, M.; Nickerson-Nutter, C. Utility of animal models for identification of potential therapeutics for rheumatoid arthritis. *Ann Rheum Dis* **2008**, *67*, 1505-1515. b) Dowty, M. E.; Jesson, M. I.; Ghosh, S.; Lee, J.; Meyer, D. M.; Krishnaswami, S.; Kishore, N. Preclinical to clinical translation of tofacitinib, a Janus kinase inhibitor, in rheumatoid arthritis. *J. Pharmacol. Exp. Ther.* **2014**, *348*, 165-173.
32. Vanhoutte, F.; Mazur, M.; Van der Aa, A.; Wigerinck, P.; van't Klooster, G. Selective JAK1 inhibition in the treatment of rheumatoid arthritis: proof of concept with GLPG0634. *Arthritis Rheum.* **2012**, *62*, Suppl 10, 2489.
33. Patil, Y. S.; Bonde, N. L.; Kekan, A. S.; Sathe, D. G.; Das, A. An Improved and Efficient process for the preparation of tofacitinib citrate. *Org. Process Res. Dev.* **2014**, *18*, 1714-1720.
34. Montero, J-L.; Dewynter, G.; Agoh, B.; Delaunay, B. Selective synthesis of sulfonylureas and carboxysulfamides. A novel route to oxazolidinones. *Tetrahedron Lett.* **1983**, *24*, 3091-3094.
35. Borghese, A.; Antoine, L.; Van Hoeck, J. P.; Mockel, A.; Merschaert, A. Mild and safer preparative method for nonsymmetrical sulfamides via N-sulfamoyloxazolidinone derivatives: Electronic effects affect the transsulfamoylation reactivity. *Org. Process Res. Dev.* **2006***, 10*, 770-775.
36. Mickelson, J. W.; Bhattacharya, S. K.; Brown, M. F.; Dorff, P. H.; LaGreca, S. D.; Maguire, R. J.; Cornicelli, J. A.; Brown, D. L.; Jennings, R.; Walker, J. K.; Huff, R. M.

Preparation of Oxadiazole Cyclobutyl Carboxylic Acid Derivatives as S1P Receptor Modulators for Treating Hyperproliferative and Autoimmune diseases. WO200960278A1, May 14, 2009.

37. Peeva, E.; Hodge, M.; Kieras, E.; Vazquez, M.; Goteti, K.; Tarabar, S.; Alve, C.; Banfield, C. Evaluation of a Janus Kinase 1 inhibitor, PF-04965842, in healthy subjects: a phase 1, randomized, placebo-controlled, dose-escalation study. *Br. J. Dermatol. 2017, in press.*doi: 10.1111/bjd.16004. Compound **25**, ***N***-{***cis***-3-[Methyl(7***H***-pyrrolo[2,3-*d*]pyrimidin-4-yl)amino]cyclobutyl}-propane-1-sulfonamide is available through MilliporeSigma (cat. no. # PZ0304).
38. $NaBH_4$ is used to minimize oxidative disulfide formation.

Figure 1: tofacitinib (**1**), baricitinib (**2**) and ruxolitinib (**3**).

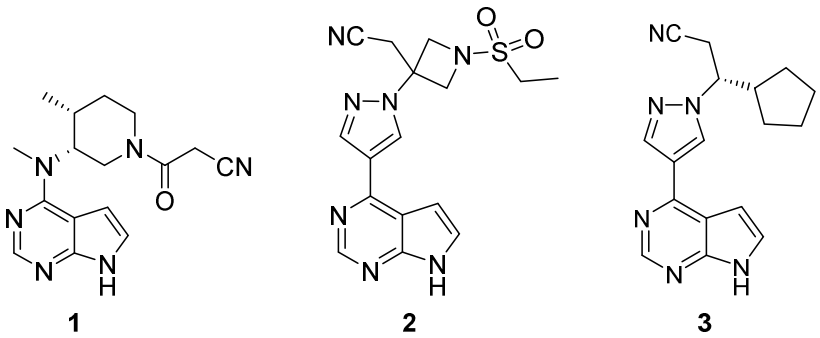

Table 1. *In vitro* biological and physical properties of sulfonamide pyrrolopyrimidine analogs.

Cmpd No.	Structure	JAK1[a] IC_{50} (μM)	JAK2[a] IC_{50} (μM)	JAK2/JAK1 ratio	HWB[b] IFNα pSTAT3 IC_{50} (μM)	HWB[b] CD34+ EPO pSTAT5 IC_{50} (μM)	HLM[c] @ 1 uM CLint, app (μL/min/mg)	LogD[d] pH 7.4
1	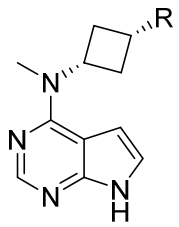	0.015	0.077	5	0.035	0.302	<8	1.1
2		0.004	0.007	2	0.029	0.088	<8	1.2
3		0.006	0.009	2	0.194	0.677	17	2.7
4	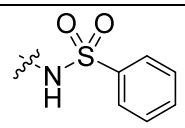	0.006	0.413	69	0.156	ND	58	2.8
5	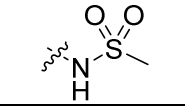	0.09	1.29	14	0.750	11.9	<8	1.2
6	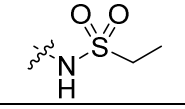	0.178	>3.31	>19	0.930	>15.9	<15	1.4
7	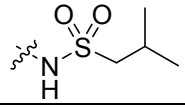	0.014	0.542	39	0.212	9.4	18	2.4
8	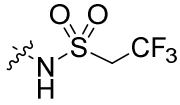	0.022	0.381	17	0.147	4.12	<10	1.9
9	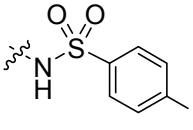	0.003	0.240	80	0.107	6.80	39	2.8
10	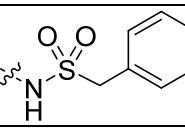	0.092	1.99	22	2.48	ND	24	2.6

[a]All compounds were assayed at 1 mM ATP at least twice and the IC_{50} averaged, with the exception of compound **10** (n = 1). [b]All compounds were assayed at least twice and the IC_{50} values averaged. [c]In vitro stability in cyropreserved human liver microsomes. [d]LogD measured between octanol/water phosphate buffered to pH 7.4.

Table 2. *In vitro* biological and physical properties of sulfamide, sulfone and reverse sulfonamide pyrrolopyrimidine analogs.

Cmpd No.	Structure	JAK1[a] IC_{50} (μM)	JAK2[a] IC_{50} (μM)	JAK2/JAK1 ratio	HWB[b] IFNα pSTAT 3 IC_{50} (μM)	HWB[b] CD34+ EPO pSTAT5 IC_{50} (μM)	HLM[c] @ 1 uM CLint, app (μL/min/ mg)	LogD[d] pH 7.4
	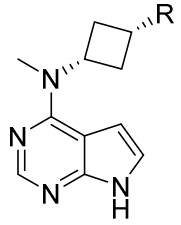							
11	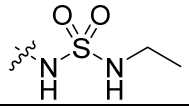	0.141	1.39	10	ND	ND	<8	1.6
12	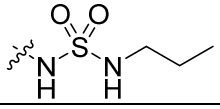	0.070	0.893	13	0.331	ND	9	2.0
13	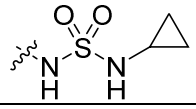	0.123	0.940	8	ND	ND	<8	1.6
14	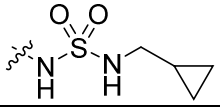	0.051	1.09	21	0.773	ND	10	2.1
15	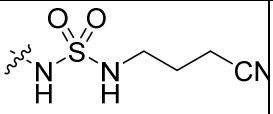	0.144	3.42	24	ND	ND	<8	1.2
16	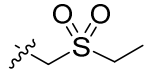	0.057	0.471	8	0.721	5.437	<8	1.2
17	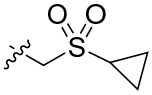	0.052	0.572	11	ND	ND	<11	1.6
18	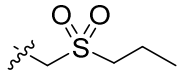	0.040	0.550	14	1.40	>20	<8	1.7
19	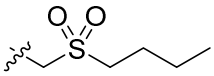	0.009	0.220	24	0.155	4.09	14	2.2
20	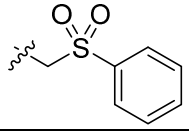	0.010	0.156	16	ND	ND	20	2.7
21	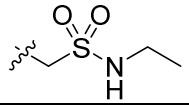	0.039	0.377	10	ND	ND	<9	1.5
22	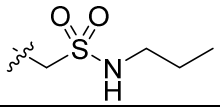	0.019	0.326	17	ND	ND	<13	2.1

23	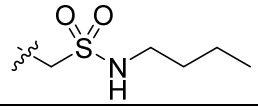	**0.030**	**0.708**	**24**	**ND**	**ND**	**47**	**2.6**
24	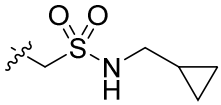	**0.011**	**0.199**	**18**	**ND**	**ND**	**18**	**2.2**

[a]All compounds were assayed at 1 mM ATP least twice and the IC_{50} averaged. [b]All compounds were assayed at least twice and the IC_{50} values averaged. [c]In vitro stability in cyropreserved human liver microsomes. [d] LogD measured between octanol/water phosphate buffered to pH 7.4.

Table 3. *In vitro* biological and physical properties of sulfonamide pyrrolopyrimidine analogs.

Cmpd No.	Structure	JAK1[a] IC_{50} (μM)	JAK2[a] IC_{50} (μM)	JAK2/JAK1 ratio	HWB[b] IFNα pSTAT3 IC_{50} (μM)	HWB[b] CD34+ EPO pSTAT5 IC_{50} (μM)	HLM[c] @ 1 uM CLint, app (μL/min/mg)	$LogD_d$ pH 7.4
25	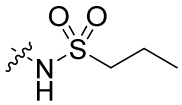	0.029	0.803	28	0.189	7.18	<9	1.9
26	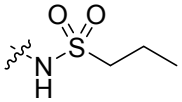 1,3-*trans* cyclobutyl	0.572	>9.297	>16	6.45	>20.0	15	2.0
27	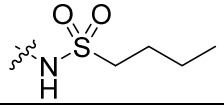	0.012	0.788	66	0.256	16.1	17	2.4
28	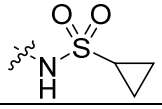	0.031	0.770	25	0.089	1.99	<8	1.6
29	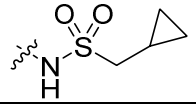	0.042	1.196	29	0.259	7.54	<8	1.8
30	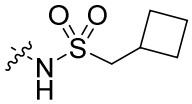	0.010	0.538	52	0.199	>20.0	31	2.4
31	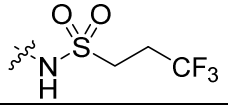	0.011	0.592	54	0.692	6.11	<8	2.4
32	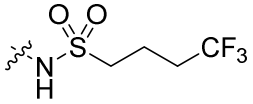	0.008	0.489	61	0.367	>20.0	<8	2.4
33	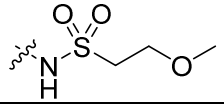	0.085	2.703	32	0.628	>15.606	<8	1.2
34	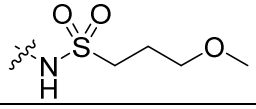	0.037	1.801	49	0.601	>15.348	<12	1.5

[a]All compounds were assayed at 1 mM ATP least twice and the IC_{50} averaged. [b]All compounds were assayed at least twice and the IC_{50} values averaged. [c] In vitro stability in cyropreserved human liver microsomes. [d]LogD measured between octanol/water phosphate buffered to pH 7.4.

Table 4: Residues differences with their location in the kinase domain of JAK1 and JAK2 structures.

Location in the kinase domain	JAK1	JAK2
Hinge	Phe958	Tyr931
Hinge	Ser961	Tyr934
Hinge	Lys965	Arg938
Hinge	Glu966	Asp939
P-loop	Glu883	Lys857
P-loop	His885	Asn859
P-loop	Lys888	Ser862

Table 5. *In vitro* biological and physical properties of "second generation" pyrrolopyrimidine analogs.

Cmpd No.	Structure	JAK1[a] IC_{50} (μM)	JAK2[a] IC_{50} (μM)	JAK2/JAK1 ratio	HWB[b] IFNα pSTAT3 IC_{50} (μM)	HWB[b] CD34+ EPO pSTAT5 IC_{50} (μM)	HLM[c] @ 1 uM CLint, app (μL/min/mg)	LogD[d] pH 7.4
35	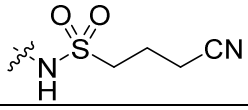	0.015	0.939	63	0.216	>6.93	<8	1.4
36	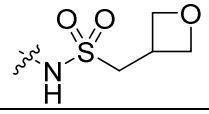	0.028	0.933	33	0.160	6.81	<8	1.0
37	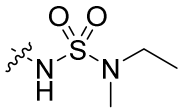	0.036	0.848	24	0.207	5.35	21	2.1
38	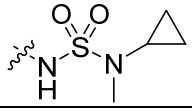	0.017	0.328	19	0.186	4.67	31	2.2
39	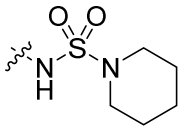	0.014	0.437	32	1.189	10.2	81	2.7
40	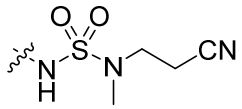	0.022	0.412	19	0.141	4.46	<8	1.3
41	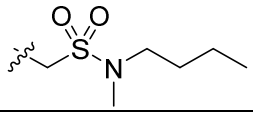	0.019	0.888	47	0.645	>20.0	117	3.0
42	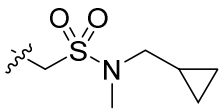	0.005	0.199	40	0.148	2.26	81	2.7
43	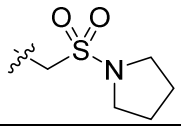	0.021	0.244	12	0.211	1.97	15	2.1

[a]All compounds were assayed at 1 mM ATP least twice and the IC_{50} averaged. [b]All compounds were assayed at least twice and the IC_{50} values averaged. [c]In vitro stability in cyropreserved human liver microsomes. [d]LogD measured between octanol/water phosphate buffered to pH 7.4.

Figure 2. X-ray crystal structure of **25** in complex with JAK1. The ligand **25** is shown in yellow. Hydrogen bond interactions of the core pyrrolopyrimidine ring with hinge residues Leu959, Glu957 and the NH group with Asn1008 are highlighted in red. The structure is of sufficient resolution (2.1 Å) to observe a bound water molecule (light pink) hydrogen bonded to N-3 of the core ring and in position to form hydrogen bond with Glu966 residue.

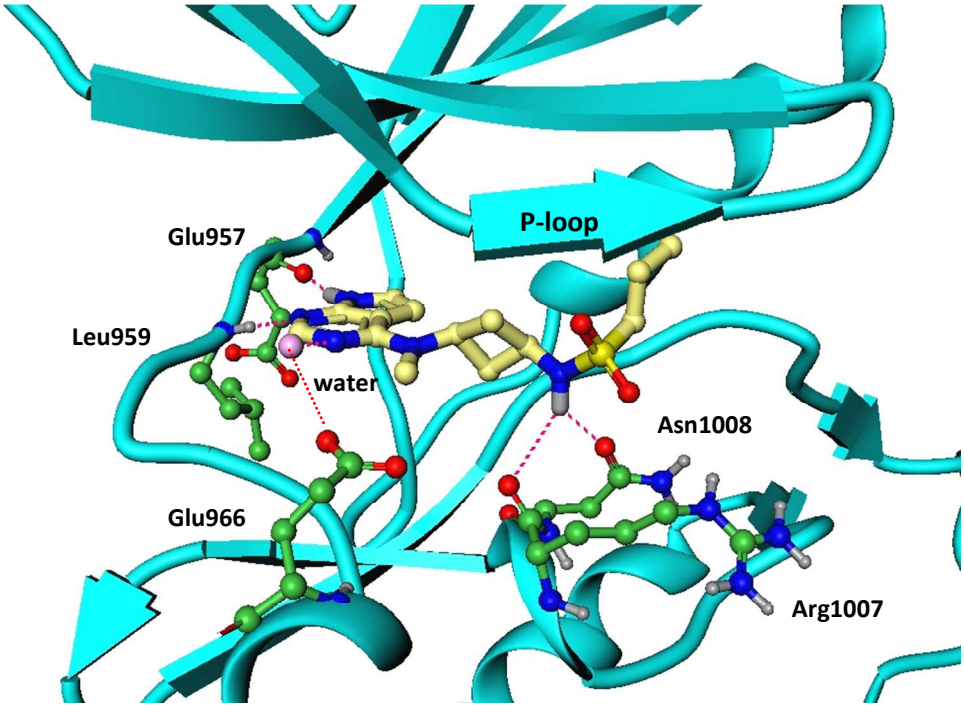

Figure 3. X-ray crystal structure of **25** in complex with JAK2. The ligand **25** is shown in magenta. Hydrogen bond interactions of the core pyrrolopyrimidine ring with hinge residues Leu932, Glu930 and the NH group with Asn981 and Arg980 are highlighted in red. The structure is of sufficient resolution(1.8 Å) to observe a bound water molecule (light pink) hydrogen bonded to N-3 of the core ring and in position to form hydrogen bond to Asp939 through a network of water molecules. For clarity, the network of water molecules is not depicted. Another water molecule is also observed forming hydrogen bond interaction with the sulfur atom of the ligand and the NH backbone of the Lys857 residue in the P-loop.

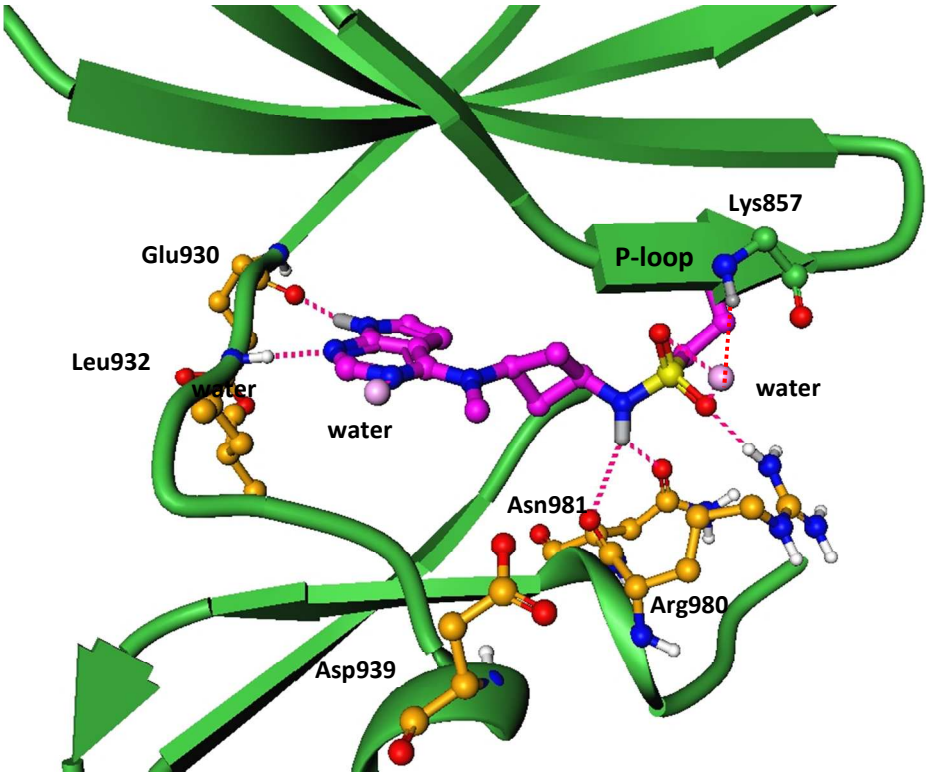

Figure 4. Orientations of the P-loops in JAK1 (cyan) and JAK2 (green) in the ligand **25** bound X-ray structures. The JAK1 bound ligand is shown in yellow, while the JAK2 bound ligand is shown in magenta.

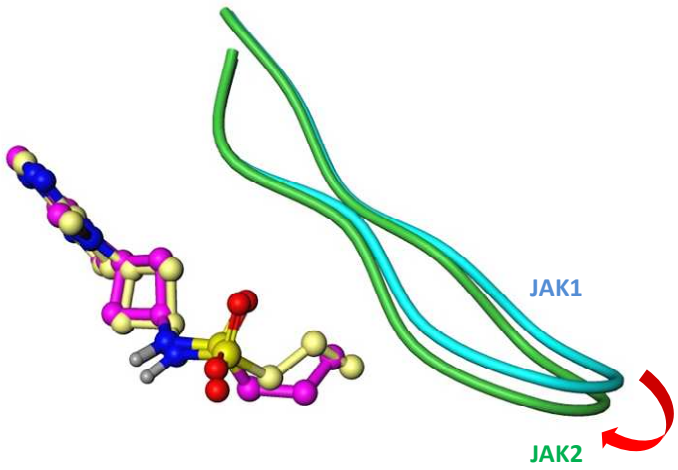

Figure 5. Torsional Profile of the dihedral (a) $S(O_2)$-C-C-C and (b) N-$S(O_2)$-C-C calculated from B3LYP/6-31G++ basis set. Green and blue arrows indicate observed dihedrals in the X-ray bound state of **25** in JAK1 and JAK2 respectively.

(a)

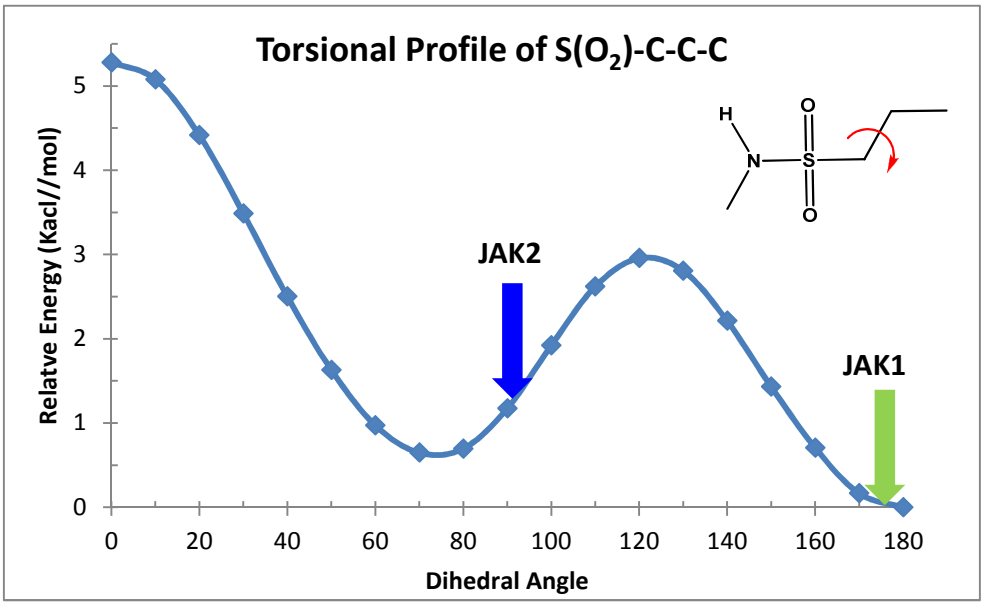

(b)

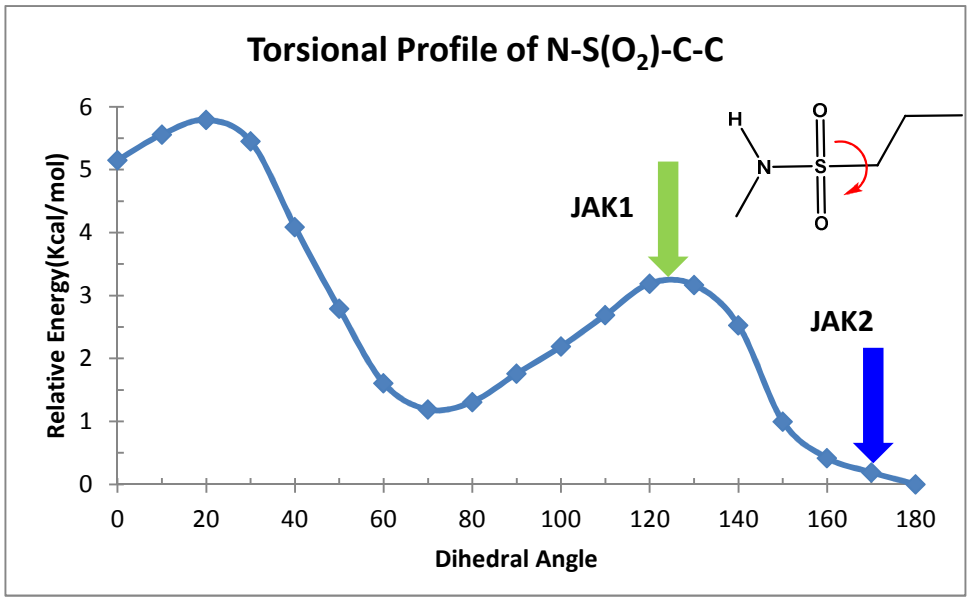

Figure 6a: Conformational preference for sulfamides. N^1 showing the s-*cis* relationship with the oxygen of the sulfone (shown in bold), while N^2 has a s-*trans* relationship with that same oxygen.

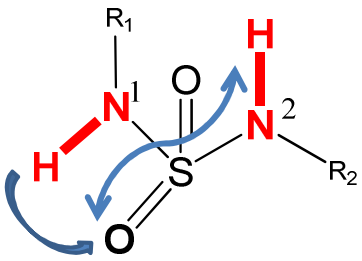

Figure 6b: Example from a CSD entry (HIXNUX) showing the s-*cis* and s-*trans* relationship in Sulfamides. Both nitrogens have pyramidal character.

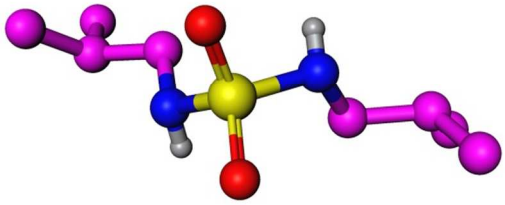

Table 6. Physicochemical properties and pharmacokinetic parameters of JAK1 inhibitors **19**, **25**, **35** and **36** in rat (n = 2) following doses of 1 mg/kg IV or 3 mg/kg p.o.

Compound	CL (mL/min/kg)	Vdss (L/kg)	$T_{1/2}$ (hours)	Oral Bioavailibility (%)	LE[a]	LipE[b]	TPSA (Å^2)	HBD	HBA	Aqueous solubility_pH7.4 (μM)	HLM CLint, app (μL/min/mg)	RRCK[c] Papp AB (10^{-6} cm/sec)
19	14.6	0.74	0.92	119	0.49	5.9	87	1	4	213	14	23
25	26.6	1.04	1.1	95.6	0.48	5.6	99	2	4	503	<9	16
35	56.4	1.42	1.3	61.1	0.46	6.4	123	2	4	259	<8	4
36	44	1.99	1.9	48.3	0.44	6.6	108	2	5	437	<8	3

[a]Ligand efficiency = (–1.4logIC_{50}(JAK1(biochemical)))/(number of heavy atoms).
[b]Ligand-lipophilicity efficiency = (–logIC_{50}(JAK1(biochemical)))/(measured logD)
[c]Apparent permeability as measured in an RRCK assay

Figure 7. Inhibition of cytokine induced STAT phosphorylation (pSTAT) in whole blood of rats dosed orally with **25.** Naïve Lewis rats were given a single dose of **25** at 50, 15 or 5mg/kg and peripheral blood taken at 0.25, 0.5, 2, 4, 8 and 24hrs post dose. STAT phosphorylation was assayed at each time point by stimulation with relevant cytokines (A) IFNγ, (B) IL-21 and (C) IL-6 then subsequent measurement of appropriate pSTATs performed. Intracellular STAT3 and STAT1 phosphorylation was determined within a CD3+ gate representing the T cell population. Data are presented as compared to maximal response in vehicle dosed animals.

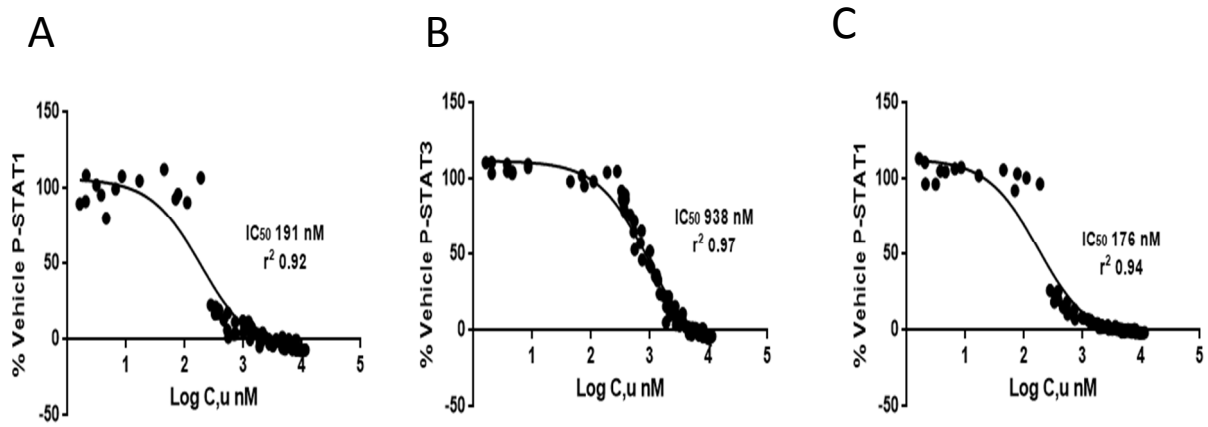

Figure 8. Rats with AIA were treated with 15, 5, 1, or 0.5 mg/kg of **25**, or vehicle control. A significant reduction of hind paw swelling was seen on: Day 3-Day 7 (15 mg/kg); Day 4-7 (5 mg/kg); Day 6 and 7 (1 mg/kg).

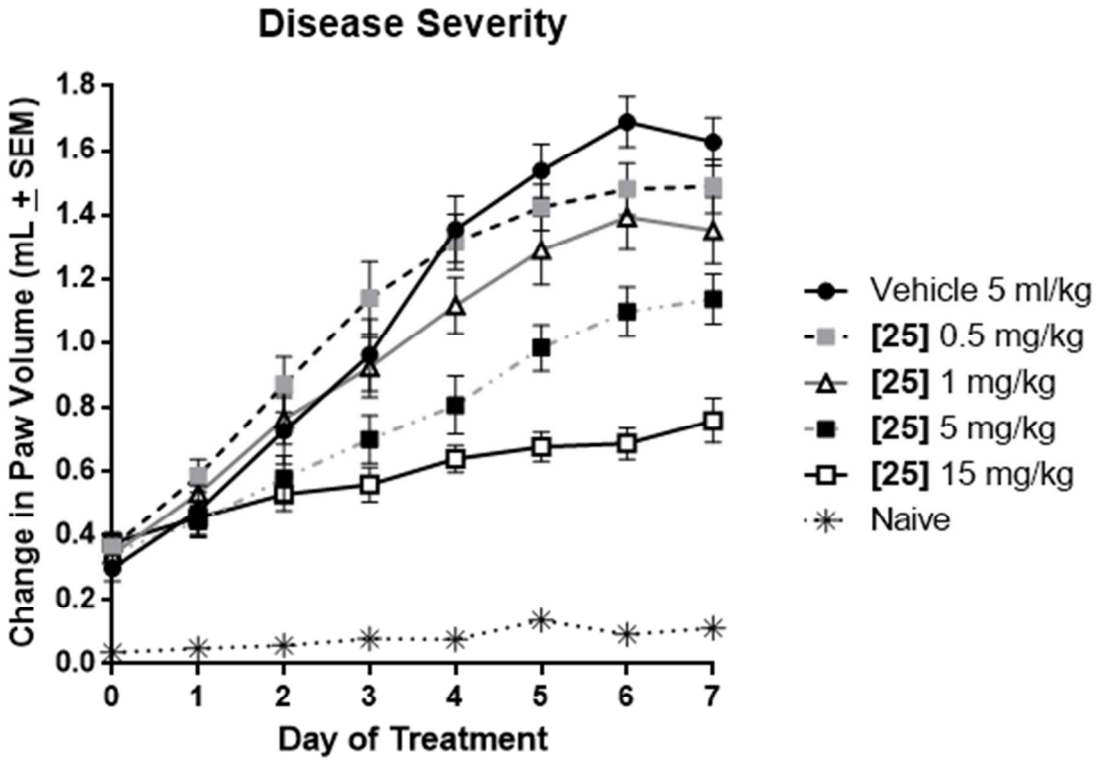

Figure 9. PK/PD modeling of exposure (C_{ave}) and its AUC of effect of **25** after 7 days of dosing in the rat AIA model. The unbound $EC_{ave}50$ concentration was determined to be 1.3 μM.

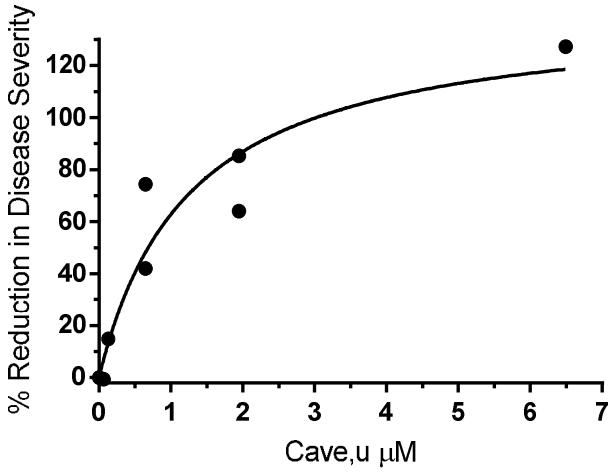

Table 7. Summary of predicted human pharmacokinetics of **25** from *in-vivo* and *in vitro* systems.

Method	Human Prediction	
	CLb (mL/min/kg)	Vss (L/kg)
Human Liver Microsomes	< 2.4	
Human Hepatocytes	5.7	
Rat Single Species Scaling	6.5	1.0
Dog Single Species Scaling	2.6	1.2

CLb: blood clearance; Vss: volume of distribution at steady state
Unbound plasma protein binding consistent across rat, dog, and human: ~0.4

Figure 10. Extent of cytokine inhibition resulting from an expected efficacious dose of **25** (200 mg QD) in human (p-STAT abbreviated as ST).

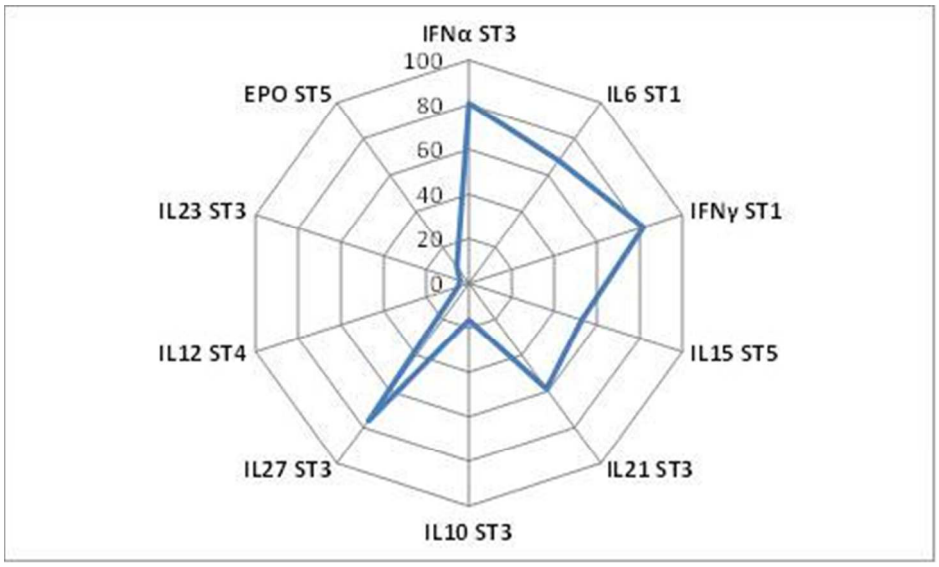

Table 8. Cytokine inhibition profile of **25** in HWB: IC_{50} values and number of repeats (n).

Compound	IFNα[a] pSTAT3 IC_{50} (μM) (n=4)	IFNγ[b] pSTAT1 IC_{50} (μM) (n=2)	CD14+ IL-6[c] pSTAT1 IC_{50} (μM) (n=4)	IL-10[d] pSTAT3 IC_{50} (μM) (n=2)	CD8+IL-15[e] pSTAT5 IC_{50} (μM) (n=5)	IL-21[f] pSTAT3 IC_{50} (μM) (n=2)	IL-27[g] pSTAT3 IC_{50} (μM) (n=2)	IL-12[h] pSTAT4 IC_{50} (μM) (n=2)	IL-23[h] pSTAT3 IC_{50} (μM) (n=1)	$CD34^+$ EPO[i] pSTAT5 IC_{50} (μM) (n=5)
25	0.189	0.163	0.163	2.511	1.298	0.511	0.271	13.673	>16.452	7.178

[a,d]Signals through JAK1/TYK2. [b,g]Signals through JAK1/JAK2. [c] Signals through JAK1/JAK2 or TYK2. [e,f]Signals through JAK1/JAK3. [h]Signals through JAK2/TYK2. [i]Signals through JAK2/JAK2.

Scheme 1. Synthesis of sulfonamide and sulfamide analogs.

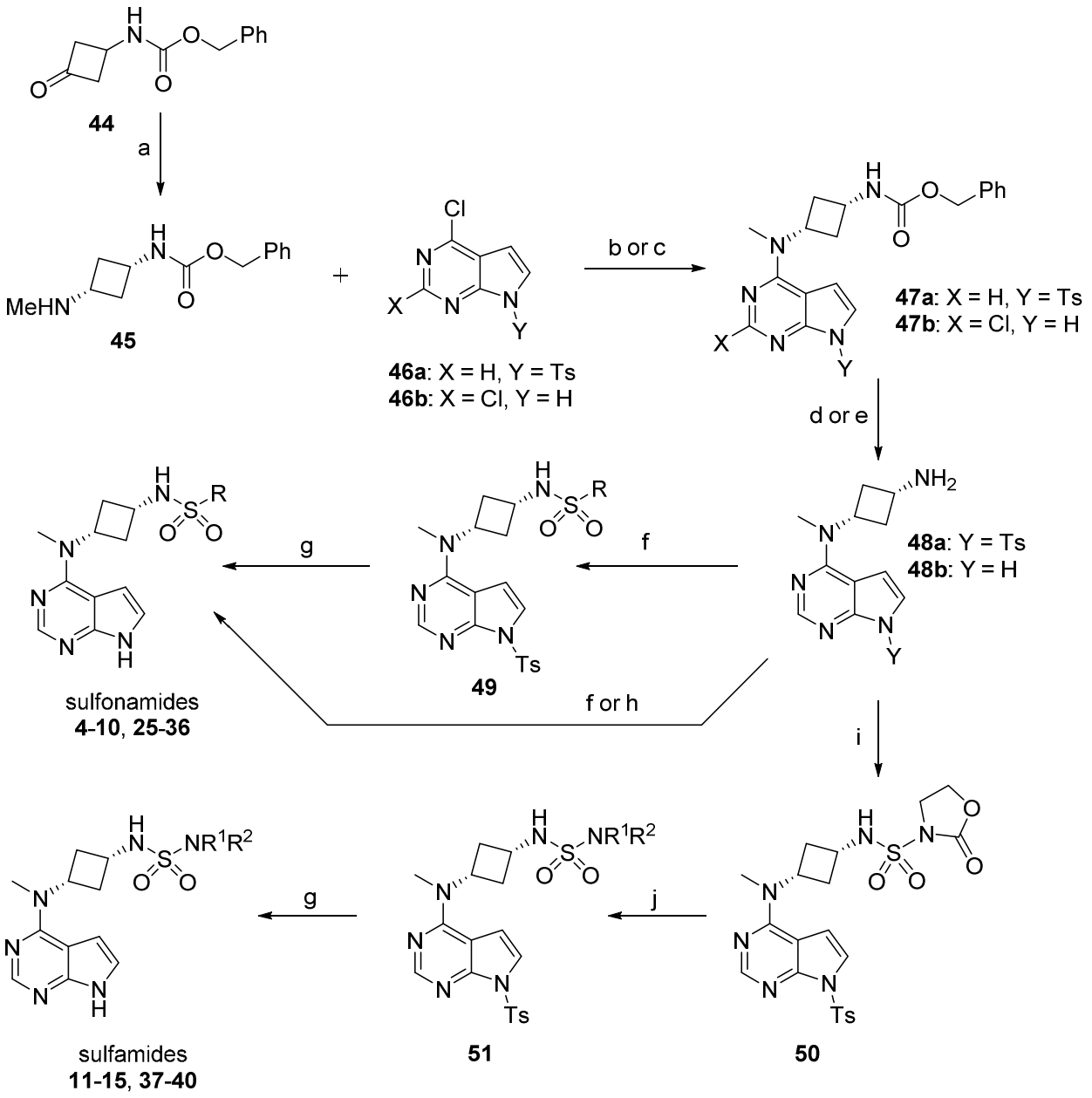

a) **44**, $MeNH_2$, THF, AcOH, rt then $NaBH_4$, 0°C to rt; b) ***cis*-45**, **46a**, DIPEA, *i*-PrOH, 75°C; c) **46b**, ***cis*-45**, K_2CO_3, H_2O, 95°C; d) **47a**, HBr, AcOH, EtOAc, rt; e) **47b**, $Pd(OH)_2$, cyclohexene, EtOH, 78°C; f) RSO_2Cl, TEA or DIPEA; g) aq. OH^- or CO_3^{2-}/ROH; h) **48b**.HCl, LiHDMS, TMSCl, rt then RSO_2Cl, rt; i) $ClSO_2NCO$, 2-bromoethanol, DCM, 0°C then **48a**.2HBr, TEA, rt; j) R^1R^2NH, TEA or DIPEA, MeCN, 100°C (sealed tube).

Scheme 2. Synthesis of sulfone and reverse sulfonamide analogs.

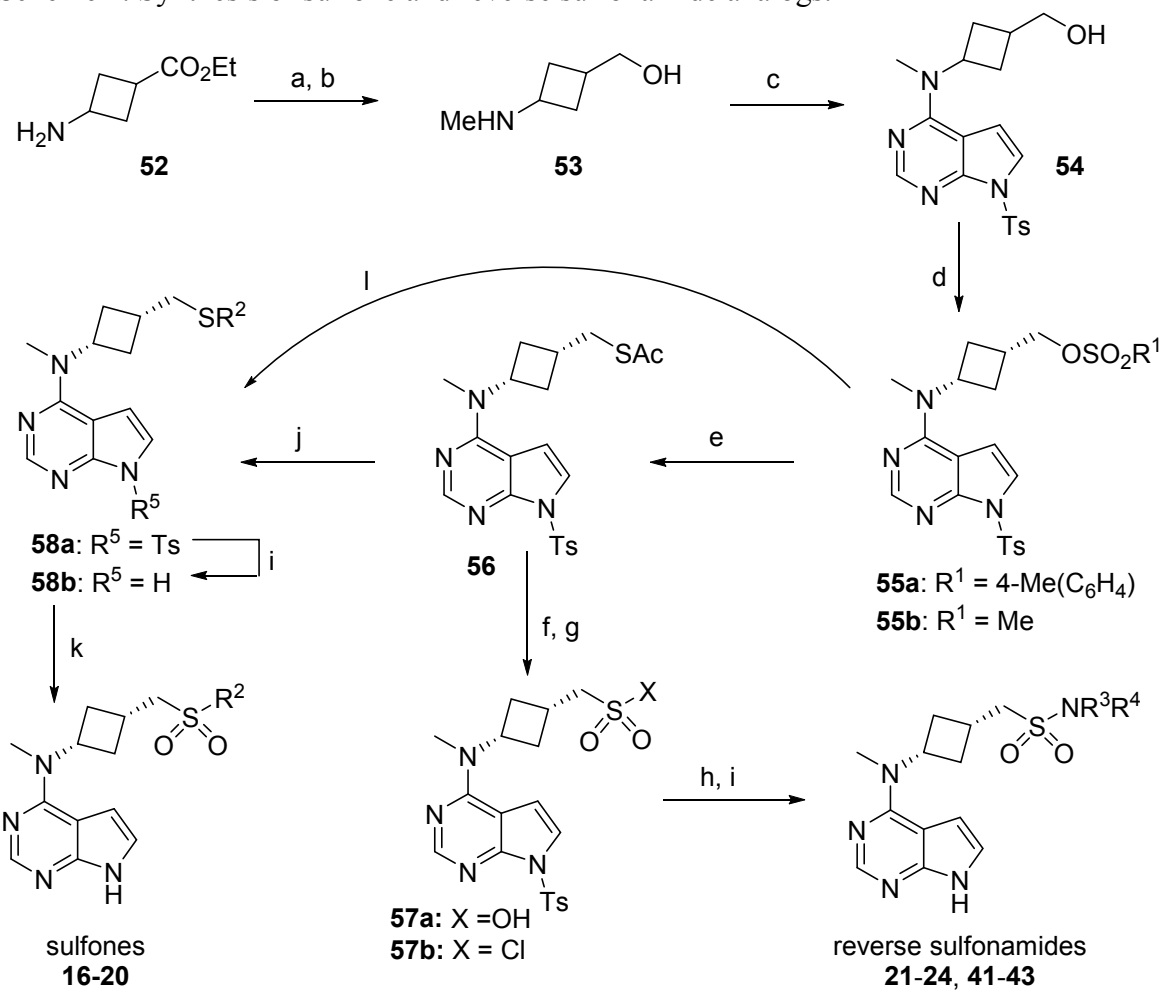

a) **52**·HCl, Boc_2O, TEA, DCM, 0°C to rt; b) $LiAlH_4$, THF, 0°C to 66°C; c) **46a**, **53**, TEA, cat. KI; d) *p*-TsCl, DMAP, DCM, 0°C to rt; e) KSAc, DMF, 55°C; f) 30% aq. H_2O_2, HCO_2H; g) $SOCl_2$, cat. DMF, DCM, 0°C to 75°C; h) R^3R^4NH, TEA or DIPEA; i) aq. OH^- or CO_3^{2-}/ROH; j) K_2CO_3, MeOH, 0°C then R^2-X, rt; k) Oxone®, THF, EtOH, H_2O; l) R^2SH, DBU, NMP, rt.

Table of Contents graphic

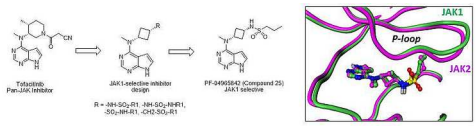

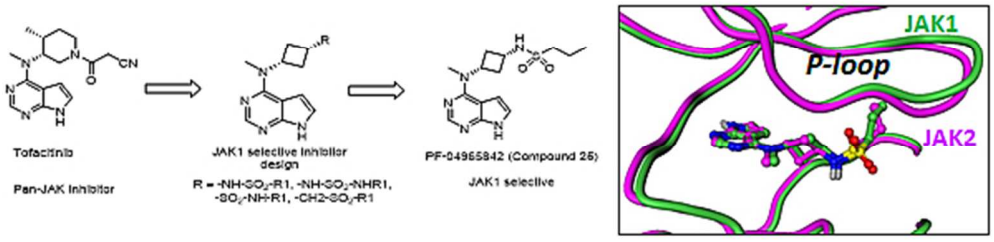

51x20mm (300 x 300 DPI)